European Journal of Agronomy 170 (2025) 127753

Contents lists available at ScienceDirect

European Journal of Agronomy

journal homepage: www.elsevier.com/locate/eja

Pedotransfer functions and their impact on soil water dynamics simulation and yield prediction: A HERMES model case study

Pablo Rosso [a,*], K.-Christian Kersebaum [a,b,c], Jannis Groh [d,e,f], Horst H. Gerke [g], Kurt Heil [h], Robin Gebbers [i]

[a] Leibniz Centre for Agricultural Landscape Research (ZALF), Data Analysis and Simulation, Eberswalder Str. 84, Müncheberg 15374, Germany
[b] Global Change Research Institute, Academy of Sciences of the Czech Republic, Bělidla 986/4a, Brno 603 00, Czech Republic
[c] Tropical Plant Production and Agricultural Systems Modelling (TROPAGS), Department of Crop Sciences, Georg-August-University of Göttingen, Grisebachstr. 6, Göttingen 37077, Germany
[d] Institute of Crop Science and Resource Conservation – Soil Science and Soil Ecology, University of Bonn, Karlrobert-Kreiten-Strasse 13, Bonn 53115, Germany
[e] Institute of Bio, and Geoscience (IBG-3, Agrosphere), Forschungszentrum Jülich GmbH, Wilhelm-Johnen-Straße, Jülich 52428, Germany
[f] Leibniz Centre for Agricultural Landscape Research (ZALF), Landscape Functioning, Isotope Biogeochemistry and Gasfluxes, Eberswalder Str. 84, Müncheberg 15374, Germany
[g] Leibniz Centre for Agricultural Landscape Research (ZALF), RA1 "Landscape Functioning", Eberswalder Str. 84, Müncheberg 15374, Germany
[h] Chair of Plant Nutrition, Chair of Ecological Farming, Technical University of Munich, Weihenstephaner Steig 22, Freising-Weihenstephan 85350, Germany
[i] Leibniz Institute for Agricultural Engineering and Bioeconomy, Agromechatronics Department, Max-Eyth-Allee 100, Potsdam D-14469, Germany

ARTICLE INFO

Keywords:
Soil texture
Field capacity
Wilting point
Water retention parameters
Crop model
HERMES

ABSTRACT

Pedotransfer functions used to determine water retention parameters from more readily available soil attributes (texture, soil organic carbon) may have a big impact on soil water dynamics and yield simulations by crop models. In this study we used the model HERMES to quantify and understand the impact of seven pedotransfer functions and two pedotransfer function ensemble models on crop yield on sites with variable texture using water retention parameters (i.e. field capacity, wilting point and total pore space) derived from the pedotransfer functions. Additionally, a continuous synthetic soil database was created to assess the effect of gradual changes in soil texture on yield simulation. The accuracy of the soil water dynamics simulations with the different pedotransfer functions was determined using soil water measurements at the test sites. The impact of pedotransfer functions on yield simulations was assessed by quantifying the yield differences at the experimental sites and across the synthetic soil database. The choice of pedotransfer functions resulted in most cases in measurable differences in soil water content dynamics, often showing a direct relationship between field capacity and water content. Often, pedotransfer functions producing higher estimated field capacity also resulted in higher yield, indicating that model yield simulation is sensitive to soil water availability. Pedotransfer functions showed an increasing variability in water retention parameters estimation and yield simulation at specific points in the sand percent continuum of the synthetic soil database, indicating that these functions can be sensitive even to small changes in particle size distribution.

1. Introduction

The dynamics of water availability for plant growth is particularly important for understanding and simulating vegetation and crop development, especially during the growing season. In process-based crop models the simulation of soil water dynamics and soil water availability to plants constitutes a central aspect. Modeling of the water dynamics in soil requires the quantification of input fluxes, such as precipitation and irrigation, the redistribution of water in the soil, and the outputs, such as evapotranspiration and drainage. Critical for the prediction of crop growth and development is the accuracy of the simulation of soil moisture dynamics in space and time (El Sharif et al., 2015; Lu et al., 2021).

Soil moisture dynamics to simulate crop growth can be estimated by

* Corresponding author.
E-mail addresses: pablo.rosso@zalf.de (P. Rosso), ckersebaum@zalf.de (K.-C. Kersebaum), j.groh@fz-juelich.de (J. Groh), hgerke@zalf.de (H.H. Gerke), kheil@tum.de (K. Heil), rgebbers@atb-potsdam.de (R. Gebbers).

https://doi.org/10.1016/j.eja.2025.127753
Received 29 January 2025; Received in revised form 20 June 2025; Accepted 21 June 2025
Available online 5 July 2025

means of a physic-based approach or by a more empirical approach such as the soil capacity-based models (Jarvis et al., 2022). To the former type belong models based on the Richards equation (e.g. AGROSIM, Mirschel and Wenkel, 2007; and Expert-N, Stenger et al., 1999), which are built on two soil hydraulic functions describing the soil water retention and the unsaturated soil hydraulic conductivity, whose parameters are obtained either by measurements or by estimations based on basic properties of the soil (Pachepsky and van Genuchten, 2011; Vereecken et al., 2008). Some difficulties related to the building and parameterization of these functions have been recognized by some studies (Szabó et al., 2021; Wagner et al., 2001; Herbrich and Gerke, 2017), and some solutions based on inverse parameter estimation have also been proposed (Groh et al., 2018; Schübl et al., 2023; Vereecken et al., 2008).

Soil capacity-based models, sometimes referred to as tipping bucket models (Emerman, 1995), belong to the empirical type of approach, used to estimate water distribution and availability in soils (Weber et al., 2024). These models assume that the vertical movement of water in the soil is mostly controlled by the intrinsic soil water retention capacities, determined mainly by field capacity (FC) and wilting point (WP). Despite Jarvis et al. (2022)'s argumentation in favor of physic-based models, soil capacity-based models are still more prevalent, and although it has been argued that these models need a relatively smaller number of input parameters than the Richard equations, FC and WP are still difficult to determine or estimate (Reynolds, 2018; Wiecheteck et al., 2020).

A number of empirical functions called pedotransfer functions (PTFs) have been developed to determine these parameters from basic, more readily available soil attributes (Vereecken et al., 2016; Wagner et al., 2001), such as soil particle size distribution (texture), soil bulk density and soil organic carbon (SOC) content. According to Van Looy et al. (2017), two approaches of using PTFs can be distinguished: the parametric approach, which aims at estimating the parameters of a given soil water retention model, and the point PTF approach, which focuses on the specific points of the soil water retention curve, such as FC and WP, also known as soil water retention parameters (WRPs).

The crop model HERMES (Kersebaum, 2011, 2019), as a soil capacity-based model, calculates plant water availability at a given time by computing the extent to which the difference between FC and WP is filled with water, while the water exceeding FC is transferred to the layer underneath. Since plant growth and development in HERMES is determined by the soil water dynamics, an accurate estimation of WRPs, and hence, the choice of the most appropriate PTF, may have a big impact (Weihermüller et al., 2021).

PTFs are empirically developed and often specific to a geomorphic region or soil type (Sun et al., 2019), to specific scales, parent material and land use (Paschalis et al., 2022; Weber et al., 2024), and therefore its applicability and accuracy depend on the difference between the properties of the soils used in the development of a given PTF and the soils under study. This and other sources of uncertainty, such as the quality of input measurements and the appropriateness of relational algorithms (Sun et al., 2019), make the use of PTFs an ongoing issue in soil water modeling, which includes testing of available PTFs and developing new ones.

Testing of several PTFs (Givi et al., 2004; Wagner et al., 2001) or even tens of them (Szabó et al., 2021) against known parameter values appears as a valid way of determining their accuracy (Pachepsky and van Genuchten, 2011). However, reference parameter values are often not available. Another way to assess the appropriateness of a PTF is by means of a functional evaluation (Chirico et al., 2010; Nasta et al., 2021, Pachepsky and van Genuchten, 2011; Ramos et al., 2023). Functional evaluation entails testing the sensitivity of the different PTFs to model's target simulation outcomes (evapotranspiration, vegetation responses, crop-mediated greenhouse gases emissions, etc.) and the relative impact of PTFs on environmental variables, often at soil or climate conditions relevant to the study area or specific scenarios. This type of assessment is typically mediated by a model whose outputs are the result of applying specific soil hydrological parameters. Notice that functional evaluation does not necessarily involve PTF accuracy testing of the model's target outputs (Pachepsky and van Genuchten, 2011), such as yield. Since complex models often have more than one uncertain parameter, it is always possible that a combination of inaccurate parameters can produce apparently accurate model outputs, hence, in the words of Kirchner (2006), getting the right answers, but for the wrong reasons.

Functional evaluation focusing on uncertainty/sensitivity analyses of model outputs has been carried out on evapotranspiration, plant primary productivity, and leaf area index (Chirico et al., 2010; Paschalis et al., 2022), surface heat fluxes (Decharme et al., 2011), solute transport in soils (Moeys et al., 2012; Van Looy et al., 2017), root water uptake and evaporation (Schaap et al., 2023), and leaf area index, biomass and yield (Kar et al., 2013). The diversity of soil/crop models and the considerable number and variety of PTFs, however, makes it difficult to extrapolate results from one study to another. In previous studies, the uncertainty brought by the choice of PTFs was highly variable, sometimes the variability was a function of site characteristics (Decharme et al., 2011), sometimes as a function of soil depth and its relationship to evaporation from the soil surface or transpiration out of the soil root zone (Chirico et al., 2010). For this reason, and until a deeper understanding of the effects of PTFs on soil water balance in space and time, and on the target outputs of a certain model (or type of model) is achieved, functional evaluations are a necessary step.

As the choice of an appropriate PTF can have an impact on the WRPs used to calculate plant water availability, the HERMES crop model has included several PTFs to choose in its simulations. The main objective of this study is to quantify and understand the impact of different PTFs on crop yield in a soil capacity-based model such as HERMES. To achieve this goal, the model was applied to four sites in Germany and the resulting simulations were compared with measured data to assess a) the accuracy of the soil water dynamics simulations resulting from the WRPs and b) the uncertainty (and possible reasons) of crop productivity predictions resulting from the use of PTFs.

2. Methods

2.1. Sites and field data

In Brandenburg, Germany:

The Boossen (Boo) site (Table 1) is a privately-owned, 70 ha-size field, with predominantly sandy soils and high soil variability (Fig. 1 and Table 2). The field was cultivated in 2020 and 2021 with corn and winter rye respectively. At both years the field was uniformly fertilized. 15 sample points (simulation units; SUs) were located, distributed to cover most of the area. At each point, soil samples were taken three times each year at 0–30, 30–60, and 60–90 cm depths to determine mineral (CaCl2 extraction and spectrophotometry, ISO 14255:1998) and total nitrogen (dry combustion, DIN-ISO 13878:1998–03), SOC (dry combustion, DIN-ISO 10694:1996–08) and gravimetric water content. At the beginning of the experiment, soil samples were taken at the three

Table 1
Site characteristics.

Site	Location (Lat., Lon.)	Altitude (m a.s.l.)	Mean precipitation (mm) / air temperature (°C)	Number of simulation units
Boossen (Boo)	52.393979°, 14.462929°	77	544/9.7	15
Dedelow (Ded)	53.379266°, 13.786676°	55	486/8.4	5
Marquardt (Mar)	52.466987°, 12.956660°	81	494 /10.9	9
Duernast (Due)	48.402430°, 11.694523°	470	810 / 7.8	9

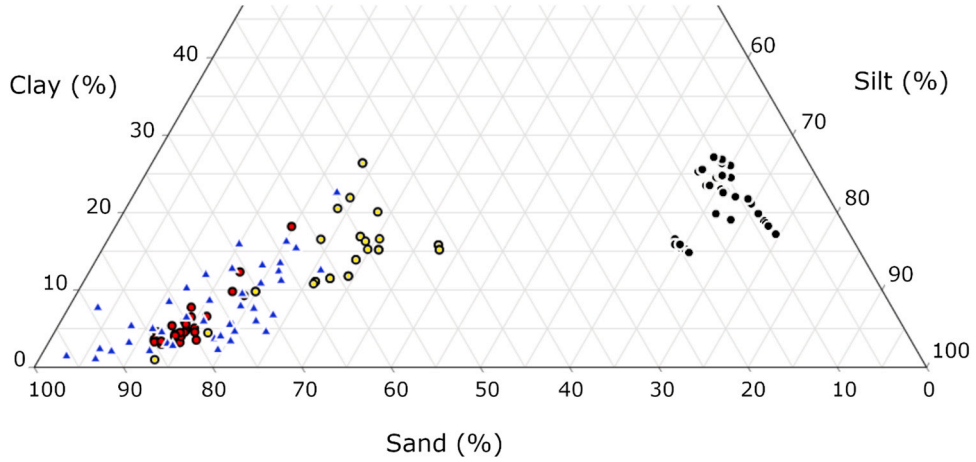

Fig. 1. Texture properties (German classification system; Eckelmann et al., 2005) of all soil layers (down to 90 or 150 cm depending on the site) and sampling units by site. Red: Marquard (Mar); blue: Boossen (Boo); yellow: Dedelow (Ded) and black: Duernast (Due).

Table 2
Ranges of soil attributes of the experimental sites. Boo: Boossen, Ded: Dedelow, Mar: Marquardt and Due: Duernast sites. SOC: Soil organic carbon.

Site	Soil type	SOC (%) (0–90 cm depth)	Bulk density (g/cm^3)
Boossen (Boo)	Sandy clay loam, sandy loam, loamy sand and sand	0.09–2.59	Not measured
Dedelow (Ded)	Clay loam, sandy clay loam, sandy loam, loamy sand and sand	0.15–1.08	1.40–1.89
Marquardt (Mar)	Sandy clay loam, sandy loam, loamy sand and sand	0.10–1.04	Not measured
Duernast (Due)	silt, silt loam and silty clay loam	0.47–1.13	1.60–1.72

mentioned depths to determine the soil particle size with the sieve-pipette method (DIN-ISO: 11277:2002). Yield was measured gravimetrically from a composite sample of three 1 m^2-quadrats around each SU.

The Dedelow (Ded) site (Table 1) consists of five lysimeters (each 1 m^2, SUs) belonging to the German wide lysimeter network TERENO-SOILCan (TERrestial ENvironmental Observatories, Pütz et al., 2016), and managed by the Leibniz-Center for Agriculture Landscape Research (ZALF in German). The soils of the lysimeters are predominantly coarse-textured and loamy (Fig. 1 and Table 2). Data from the growing seasons 2014–2018, corresponding to winter wheat (two years), winter rye (two years) and oats, were used for this study. Data used in this study are based on the soil profile approach (variable depths) and the corresponding measurements of the soil were texture, total nitrogen (see method above), SOC (see method above) and bulk density from 0 to 150 cm depth. Texture was determined with the sieving-pipette method (same methods as above). The bulk density data obtained from core samples extracted in soil profiles next to the lysimeter extraction sites (Pütz et al., 2016; Herbrich and Gerke, 2017). Soil water content was measured at three depths (10, 30, and 50 cm) every half hour using time domain reflectometry probes (CS610, Campbell Scientific North Logan, US); data was aggregated to daily values. Yield was gravimetrically measured after harvesting the entire lysimeter.

The Marquardt (Mar) site (Table 1) is an experimental field at the Leibniz Institute for Agricultural Engineering and Bioeconomy (ATB in German) located near the town of Marquardt, with predominantly sandy soils (Fig. 1 and Table 2). The field is 0.3 ha (25 m*120 m) in size subdivided into 16 rectangular plots consisting of a design of four fertilization levels with four replications, cultivated during the years 2019–2021 with winter wheat, corn and winter rye, respectively. At each plot, a central point was sampled three times each year to determine mineral (see method above) and total nitrogen (see method above), soil organic carbon (see method above) and gravimetric water content at 0–30, 30–60, and 60–90 cm soil depths. At the beginning of the experiment, soil samples were taken at the three mentioned depths to determine the soil particle size with the sieve-pipette method (DIN-ISO: 11277, 2002). Since not all the 16 plots had information for the three years, a group of nine plots (SUs) representing a high variability in soil types was used. Yield was measured gravimetrically from a 4 m^2-quadrat located at the center of each SU.

In Bavaria, Germany:

The Duernast (Due) site (Table 1) is an experimental field managed by the Technical University of Munich (Heil et al., 2018), with predominantly silty soils (Fig. 1 and Table 2). Data from nine plots or SUs (4 m*6 m each) covering a total area of about 500 m^2 including three replications at three fertilization levels: 0, 120 and 180 kg/ha of nitrogen, were used for this study. The growing periods considered were 2016–2020 during which corn, winter wheat, corn, winter wheat and spring wheat (in this latter case, no fertilizer was applied) were subsequently planted. At each plot, soil water content at 10 cm soil depth intervals down to 85 cm and from 85 to 105 cm depth was recorded daily over periods of several months using electrical capacitance sensors (EnviroSCAN, Sentek, Stepney, Australia). At the beginning of the experiment, texture at 0–30, 30–60, and 60–90 cm soil depths was determined with the sieve-pipette method (DIN-ISO: 11277, 2002). Additionally, mineral nitrogen (in NO_3 and NH_4, in kg/ha; see method above) and water (gravimetric water content) were measured at the beginning of each growing period. Due had a relatively less variable soil in terms of soil texture but showed large differences in nutrition levels due to the fertilization treatments. Yield was measured at each plot with a conventional plot combine harvester.

Yield and the developmental stages of the crops were recorded at all field sites for model calibration purposes.

2.2. The Model HERMES

HERMES (Kersebaum, 2011, 2019) is a process-based functional model designed to simulate crop growth, water, and nitrogen (N) dynamics in arable lands. The model calculates the plant water uptake by distributing the potential transpiration (as fraction of potential evapotranspiration computed from the current leaf area index) over a soil depth proportional to the root length density and the plant available water in each layer.

Reference grass evapotranspiration in HERMES can be calculated using different approaches. In this case the Turc-Wendling method (Wendling et al., 1991), a well-established method in Germany also used

by the German Weather Service, was chosen (Kersebaum, 2007). The formula is a nationally adapted modification of the TURC formula, which is ranked as number two for humid climates (Jensen et al., 1990; Smith et al., 1998) and requires the diurnal average temperature and global radiation sum. The model uses crop coefficients (kc) describing the relation between crop and reference grass evapotranspiration to calculate potential evapotranspiration specific to the crop growth stage and soil coverage. Depending on the plant available water fraction (i.e., the difference between FC and WP), a root efficiency factor is calculated, which declines with decreasing available water fraction. If the calculated uptake exceeds the available water, the deficit is distributed in the same way to deeper layers until the rooting depth is reached. Root water uptake ends at the root depth or at the first groundwater layer (whichever comes first).

Besides kc, crop variety parameters in HERMES include other properties such as CO_2 assimilation and maintenance rates, initial nitrogen content in organs, and more than 12 additional parameters for each of the six development stages, including specific leaf area, drought stress threshold and temperature sum. The temperature sum determines the time of transition from a crop development stage to the next. When not available, this parameter is set using field-based reference phenological information.

A capacity approach is used to describe soil water dynamics. HERMES calculates plant available soil water on a daily basis by computing at each soil layer the extent to which the plant available soil water storage capacity (i.e., the difference between FC and WP) is filled. Calculations are made by discretizing the soil profile into 20 layers of 10 cm each. The amount of water exceeding FC in a layer is transferred to the layer underneath. HERMES also estimates capillary rise from shallow groundwater by calculating a steady upward water flux into the bottom soil layer, limited by a critical water content of 70 % of available water. The daily flux is estimated depending on soil texture and the distance between the layer and the groundwater table, based on tabulated values (Eckelmann et al., 2005).

To calculate the plant water availability, three WRPs need to be provided: FC, WP, and total pore space (PS). HERMES has five different options for calculating the WRPs directly from measured soil properties. The four methods used in this study are shown in Table 3.

The daily net dry matter production by photosynthesis and respiration is simulated in HERMES from global radiation and temperature. Dry matter production is partitioned to crop organs depending on crop development stage. Crop yield is estimated at harvest as a defined fraction of the weight of the defined harvested organs. Water stress is calculated from the fraction of actual to potential transpiration. Water deficiency may also induce limitation of nitrogen supply due to low water uptake and low nitrogen diffusion to root surfaces leading to additional nitrogen stress.

Weather data used to feed the simulations must include at least daily maximum and minimum air temperature, daily precipitation, daily global radiation, and daily wind speed.

2.3. PTFs and WRP calculation

The first WRP estimation option in the KA5 mode in HERMES is based on a look-up table that relates the soil type class to average values of PS, FC and WP. In this case, soil input information for the modeling is provided in the form of soil category classes (i.e., "class type" of PTFs) and bulk density classes.

The other three methods, EU PTF v.1 (EU1), Batjes FC@2.5 pF (B25) and Batjes FC@1.7 pF (B17) use PTFs as described in the literature (Table 3 and Annex A). In the case of EU1, from the over 20 equations developed in the study, we used PTF 5 for PS, PTF 9 for FC, and PTF 12 for WP (see Annex A), because these are the only continuous functions to estimate these parameters. In all PTFs, the input soil information included percentages of sand, silt, clay, and soil organic carbon (SOC) content. EU1 also requires bulk density for calculating PS. The adoption

Table 3
Pedotransfer functions (PTF) tested, and the reference water retention parameter (WRP) used.

PTF Tested	Acronym	Model type Inputs	Region	Reference
Bodenkundliche Kartieranleitung. KA5 *(In HERMES)*	KA5	Class-based/ LUT. Soil category classes, bulk density classes	Germany	Eckelmann et al. (2005)
EU PTF v.1 *(In HERMES)*	EU1	Regression/ continuous. Texture, soil organic carbon, bulk density	Europe	Tóth et al. (2015), (see also Appendix A)
Batjes FC@2.5 pF *(In HERMES)*	B25	Regression/ continuous. Texture, soil organic carbon	World	Batjes, (1996), (see also Appendix A)
Batjes FC@1.7 pF *(In HERMES)*	B17	Regression/ continuous. Texture, soil organic carbon	World	Batjes, (1996), (see also Appendix A)
EU PTF v.2	EU2	Machine learning/ continuous. Texture, soil organic carbon, bulk density	Europe	Szabó et al. (2021)
Rosetta PTF (v.3)	ROS	Artificial neural network/ continuous. Texture, bulk density	North America and Europe	Zhang and Schaap, (2017)

of these three methods (i.e., "continuous" PTFs) was made under the rationale that PTFs using continuous functions may reproduce better the transition between classes and, therefore, be more appropriate for higher spatial resolution simulations for precision agriculture applications (Wallor et al., 2019).

Two additional PTFs, EU PTF v.2 (EU2) and Rosetta (ROS) (Table 3) not included in HERMES, but widely used (Weihermüller et al., 2021; Montzka et al., 2017; Krevh et al., 2023), were tested in the simulations. The PTF EU2-based soil WRPs were calculated outside Hermes using an online calculator or, for large sample sizes, a Python script developed and provided by Szabó et al. (2021). A list of soil entries containing depth, soil texture, SOC content and bulk density is provided as input and the algorithm produces PS, FC and WP values. The EU2 PTF has more than 30 algorithms that can be chosen depending on the input variables to be included. Based on the best performances obtained in Szabó et al. (2021), PTF03 was used for PS and FC (@1.8 pF), and PTF02 for WP.

WRPs corresponding to the ROS PTF were calculated by means of an R script based on the tutorial "Rosetta Model API" (Beaudette et al., 2024). Unlike the previous PTFs, which calculate WRPs directly from soil parameters, ROS builds first a water retention curve from which WRPs are derived. Also, in contrast to the other methods, ROS does not use SOC content.

Since parameters derived from multi-model predictions (or model ensembles) have proven to be an effective alternative for addressing individual model uncertainties (Guber et al., 2009) and combine the strengths of different models (Chen et al., 2024), two PTF combinations were created. In the first combination, WRPs (FC, WP and PS) from all PTFs were averaged, and in the second, the median of the WRPs was selected to combine all PTFs. These two combinations, called MEA and MED, respectively, were then used to run the HERMES model at all sites.

These model combinations, or PTF ensembles, are to be differentiated from a more typical model ensemble, in which means and other statistical parameters are obtained from the model outputs, such as yield. Since ensembles constitute an efficient way of minimizing extreme behavior of individual models, model ensembles are particularly useful when diverse models are included. In the case of this study, where only one model was used, the emphasis was placed on minimizing potential biases and inaccuracies of the PTFs tested. Therefore, PTF ensembles were preferred.

2.4. Model simulations

A total of 38 (Boo 15, Ded 5, Mar 9, Due 9) HERMES model runs were carried out with each of the seven WRP estimating methods, and the two PTF ensembles. HERMES calculates soil dynamics using discrete soil layers of 10 cm each (to 2 m of depth). Based on the soil information available for each site, soil texture, SOC, carbon-N ratio and bulk density were input in three groups of layers (0–30, 30–60 and 60–90 cm) at Boo, Mar and Due, and in variable groups of layers at Ded based on the characteristics of each SU soil profile. To complete the soil information down to 2 m, values from the deepest layer with available information were used, except for SOC which was assumed to be zero.

For Ded, a time series of distances to groundwater table depth, derived from matric potential measurement using tensiometer (TS1 tensiometer, UMS, Munich, Germany) at 1.4 m soil depth, ground water measurements were used as lower boundary condition. Based on field manager's experience and records from close-by stations a constant ground water table depth of 2 m was chosen for Mar and Due. For Boo, the ground water table was assumed to be deep enough to not influence the soil water balance (a value of 9.9 m in HERMES) was used. Bulk density in HERMES is entered in the form of classes. At Boo and Mar, where no measurements were available, a default class 2 (1.4–1.6 g/cm^3) was assigned to the 0–30 cm layer and a class 3 (1.6–1.8 g/cm^3) to the rest of the layers. After a first run, the available phenology information from the field was used to calibrate the model adjusting the temperature sum requirements of each development stage. Weather data was obtained from nearby weather stations.

2.5. Testing of PTF performance

Except for the site Ded, there were no independent estimates of FC and WP available. Therefore, testing of the simulated WRPs was done by comparing the soil water dynamics simulations with observed soil water content time series at each site. This led to an assessment of both the relative accuracy and the sensitivity of the simulations with respect to each WRP. At Boo, Mar and Due measurements and simulation results were grouped in three soil layer depths: 0–30, 30–60 and 60–90 cm. The average water content of each layer group was used to compare with equally averaged measured.

At Ded, 10 cm (a HERMES simulation soil layer) above and below the 10 and 50 cm water measuring depths (0–20 and 40–60 cm, respectively) were averaged. Since at around 30 cm of depth there was a change in horizon in all soils, soil water simulations at the layer 20–30 cm were used to compare with the 30 cm reflectometry measurements. Independent estimates of WRPs at Ded were done on soil core samples with the HYPROP soil moisture release device.

Accuracy of the PTF-generated soil water content dynamics was assessed by comparing soil water content measurements against simulated values date by date. At sites Ded and Due, dense time series of measured soil water content (150–300 measurements per year) were available, whereas at Boo and Mar soil water content was available three times per year.

Forty-five metrics from the "metrica" R package (Correndo, 2024) were calculated to compare measured with predicted water content. Most of these performance metrics can be separated into methods that measure accuracy (concordance between simulations and measurements) such as the Pearson's correlation coefficient or the concordance correlation coefficient; and methods that measure error (departure of simulations from measurements), such as the mean absolute error, the relative absolute error or the relative squared error. Among the error metrics, the mean absolute scaled error (MASE; Eq. 1) is particularly suited for time series (Correndo, 2024), because it scales the error using the residuals of the two consecutive measured values (random walk method, Hyndman and Koehler, 2006).

$$\mathrm{MASE} = 1 \Big/ n \left(\frac{|M_i - P_i|}{\frac{1}{T-1}\sum_{t=2}^{T} |M_t - M_{t-1}|} \right) \quad (1)$$

where M is measured, P is predicted, and T is time.

The widely used mean absolute error (MAE) is also absolute, but not scaled, and therefore, lacks the denominator of Eq. (1).

Signed measurements of error such as the percentage bias error (PBE, Eq. (2)) are particularly useful to indicate prediction bias (systematic error) to distinguish over- from underestimation of predictions.

$$\mathrm{PBE} = 100 \left(\frac{\sum (M_i - P_i)}{\sum M_i} \right) \quad (2)$$

where M is measured, and P is predicted.

The fact that PBE is calculated as percent of the measured value, it was assumed to be well suited for comparison among sites in this study.

Metrics obtained at all depths and SUs were pooled together to obtain a single statistics per site.

2.6. PTFs and yield simulation

Results of the model simulations with all the PTFs were used to study the relative impact of the WRP estimates on yield prediction. The most important criterion to assess the significance of the PTF effects was to determine how the resulting yields differ with respect to crop, year, crop field management (treatments) and soil properties. To this end, a) yield averages of each PTF for all the plots per year and b) averaged coefficients of variation (CV) of all PTF-based yields per site year were calculated. CV was calculated as the standard deviation of the PTF-based yields at each SU (plot), standardized by the mean PTF yields of that SU. Then CVs were averaged per year. A one-way ANOVA was calculated for each year at each site to test the statistical significance of simulated yield differences among PTFs.

2.7. Soil texture and PTFs

To explore the possibility that differences in PTF performance might have to do with differences in soil texture, a synthetic soil texture database was used to simulate yield with the different PTFs. A total of 25 soils with increasing sand proportion from 50 % to 98 % (2 % increment steps) and decreasing clay percent from 25 % to 1 % was created. Silt proportion was set to add up to 100 % keeping its percent as fixed as possible at 25, 20, 15, 10 and 5 to 1 % as sand content increased (Fig. 2). These texture values were assigned equally to all soil layers. This particular texture configuration of medium to high sand and medium to low clay was chosen to account for the conditions of the soils of the three sites in Brandenburg, from where most of the data originated. Soil organic carbon default values of 1.0, 0.5, 0.2 and 0.0 (%) at the layers 0–30, 30–60, 60–90 and 90–200 cm respectively were assigned to all soils. WRPs were estimated for each of the 25 soils using the different PTFs. Crop varieties and weather from Boo were used to simulate yield with HERMES for each PTF.

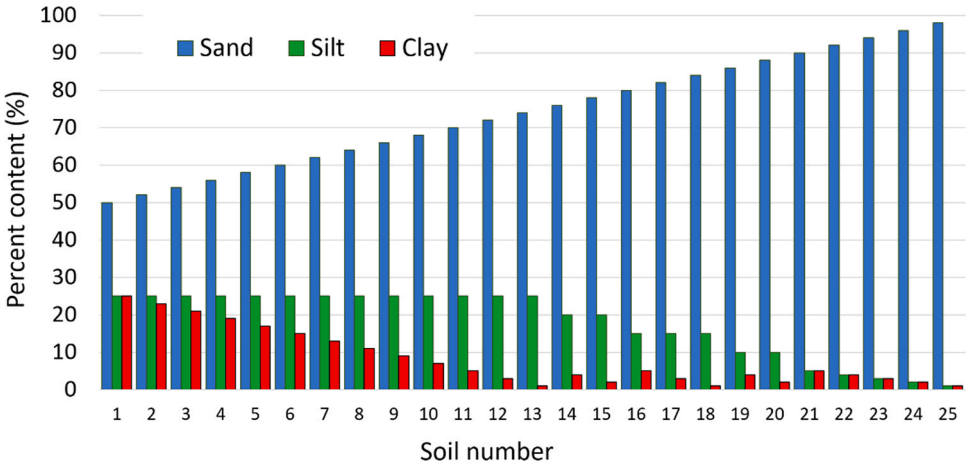

Fig. 2. Sand, silt and clay content used at all soil depths of the synthetic soil database.

3. Results

3.1. Soil water retention parameters

PTFs produced variable WRPs at Boo (Fig. 3), Mar (Fig. 4) and Ded (Fig. 5), but relatively uniform at Due (Fig. 6), which is also reflected in the texture variability of the sites (Fig. 1). PTFs at all sites showed a consistent pattern in which KA5, EU1 and EU2 tended to be among the highest FC values (around 20 % soil volume or higher at Boo and Mar), and B25, B17 and ROS among the lowest (around 10 % soil volume at Boo and Mar). The degree of variability in FC appeared to be higher than in WP, therefore differences in FC also are expected to strongly influence the levels of soil available water capacity (AWC). A comparison between some of the simulated WRPs from Fig. 5 and the HYPROP-estimated

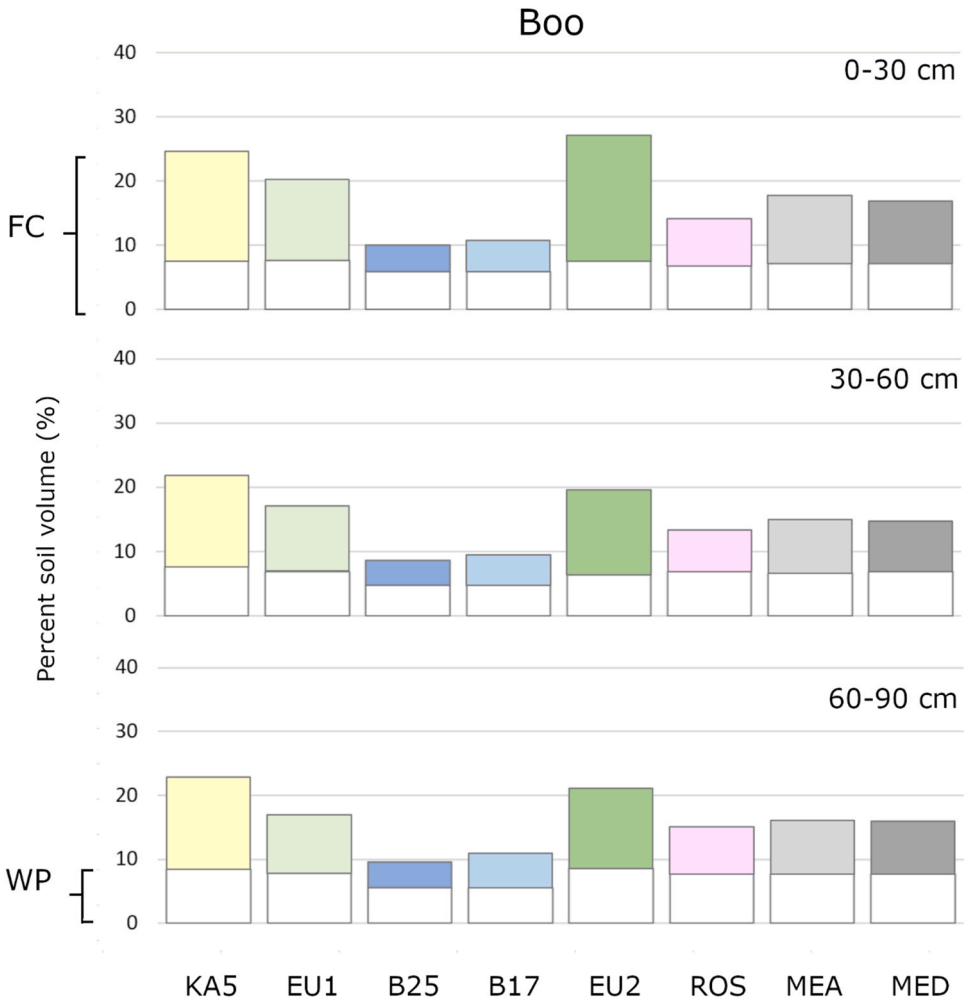

Fig. 3. Boo site average of field capacity (FC, total bar height) and wilting point (WP, white bars) at different soil depths predicted by each PTF (KA5, EU1, B25, B17, EU2 and ROS) and the PTF ensembles (MEA and MED). Color bars indicate soil available water capacity (AWC). (Colors were chosen only to enhance visualization).

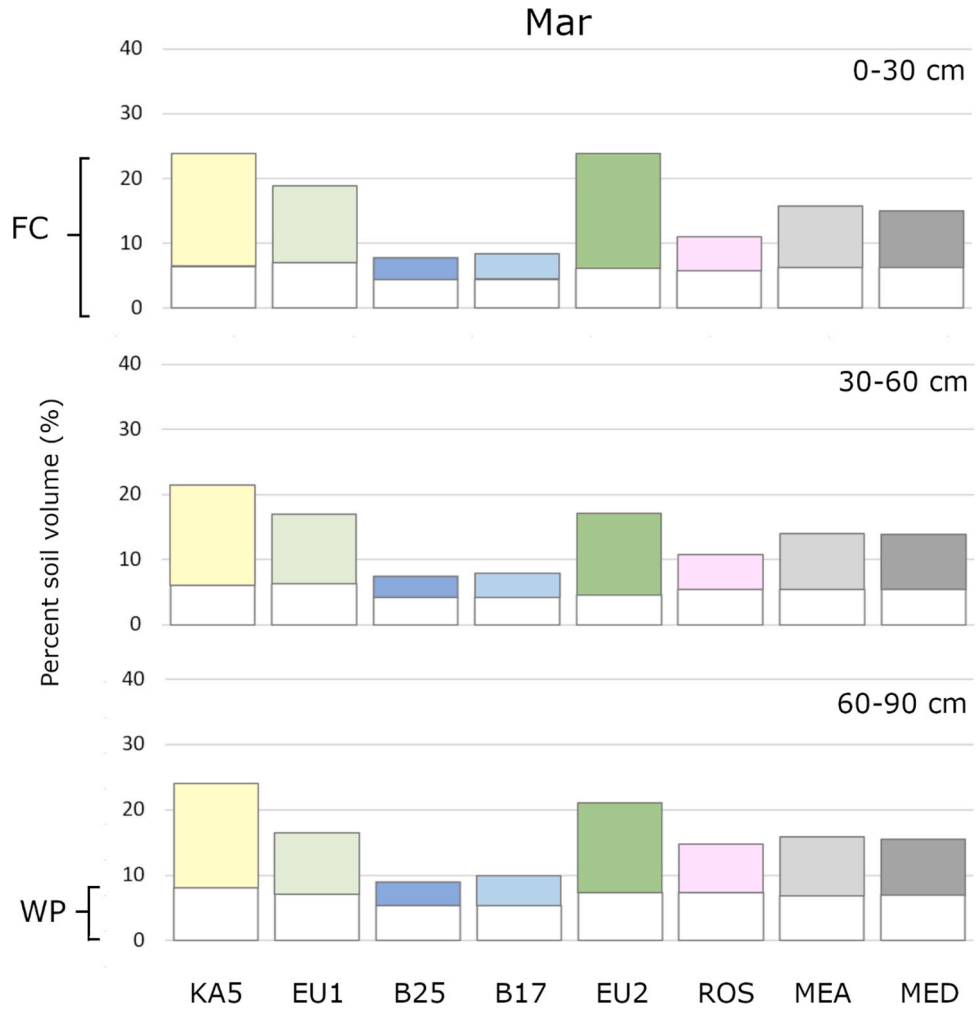

Fig. 4. Mar site average of field capacity (total bar height) and wilting point (white bars) at different soil depths predicted by each PTF (KA5, EU1, B25, B17, EU2 and ROS) and the PTF ensembles (MEA and MED). Color bars indicate soil available water capacity (AWC). (Colors were chosen only to enhance visualization).

WRPs at Ded (Fig. 7), showed a tendency of HYPROP to assign relatively high PTFs but lower WP, resulting in a relatively higher AWC than the other PTFs.

3.2. Testing of soil water content

All error metrics in this study showed a similar behavior at all sites. This means that the ranking of PTF performance and their relative accuracy was stable across metrics, as can be exemplified by the Ded results (Fig. 8), where each PTF performed similarly with respect to the other PTFs according to MASE, MAE and PBE metrics.

Boo and Mar had relatively sparse measured values (three per year) and as a consequence, the scaling factor in MASE based on consecutive measurements was not representative of the rate of change in soil water content. Therefore, and since MASE and MAE produced almost identical results, MAE was chosen to be the error metric shown in the results.

No single PTF performed best across all sites (Table 4). B25, B17, MEA and MED were the only methods that ranked among the best three on more than one site. At Due all PTFs performed similarly and with higher errors than at the other sites. Considering sites individually, at Boo, the methods with lower error (MAE values of 4.09–4.43 % soil volume; versus highest MAE of 8.15 %) corresponded to PTFs with intermediate FCs (Fig. 3) and relatively lower AWC. At Mar, the best performing PTFs (MAE values of 2.33–2.47 % soil volume; versus highest MAE of 5.09 %) were the methods with the lowest FC and reduced AWC (Fig. 4). At Ded, similarly to Boo, the best methods (MAE values of 4.09–4.43 % soil volume; versus highest MAE of 8.65 %) showed intermediate WRPs (Fig. 5); and at Due, the best performing methods (MAE values of 6.76–7.70 % soil volume; versus highest MAE of 9.11 %) were among the PTFS with the higher FC and AWC (Fig. 6).

In cases where PTFs with the lowest MAE did not match those with the PBE closest to zero (as in ROS vs. MEA at Boo and EU2 vs. MEA at Ded), it can be inferred that there was a larger component of random error (that is cancelled by the sign of the error) than of bias.

When observing the soil water dynamics (e.g., Fig. 9), all PTFs appear to follow a similar pattern of high and low water content while showing the highest differences between PTFs during the winter months, which are characterized by higher water contents. At this time, when there is little water use by plants and temperatures are low, soils tend to stay at maximum water capacity, and HERMES tends to set these water content values close to FC. Therefore, soil water maxima for the different PTFs resemble the FC averages presented above (e.g., compare Figs. 3 with 9).

In the case of Boo (Fig. 9), although only a few measuring points were available, measured water content seemed to be well represented by the simulated increases and decreases in water content, with the absolute values of measurements being closer to the PTFs that showed better overall accuracies (MEA, MED, B17 and ROS, Table 4). At deeper layers (Fig. 10), all PTFs showed similar high and low water content patterns except at the late summer period (July-October 2020) when soils are being rewetted. In the case of PTFs producing higher FC values, soils tended to be rewetted later in the season than for PTFs with low FC.

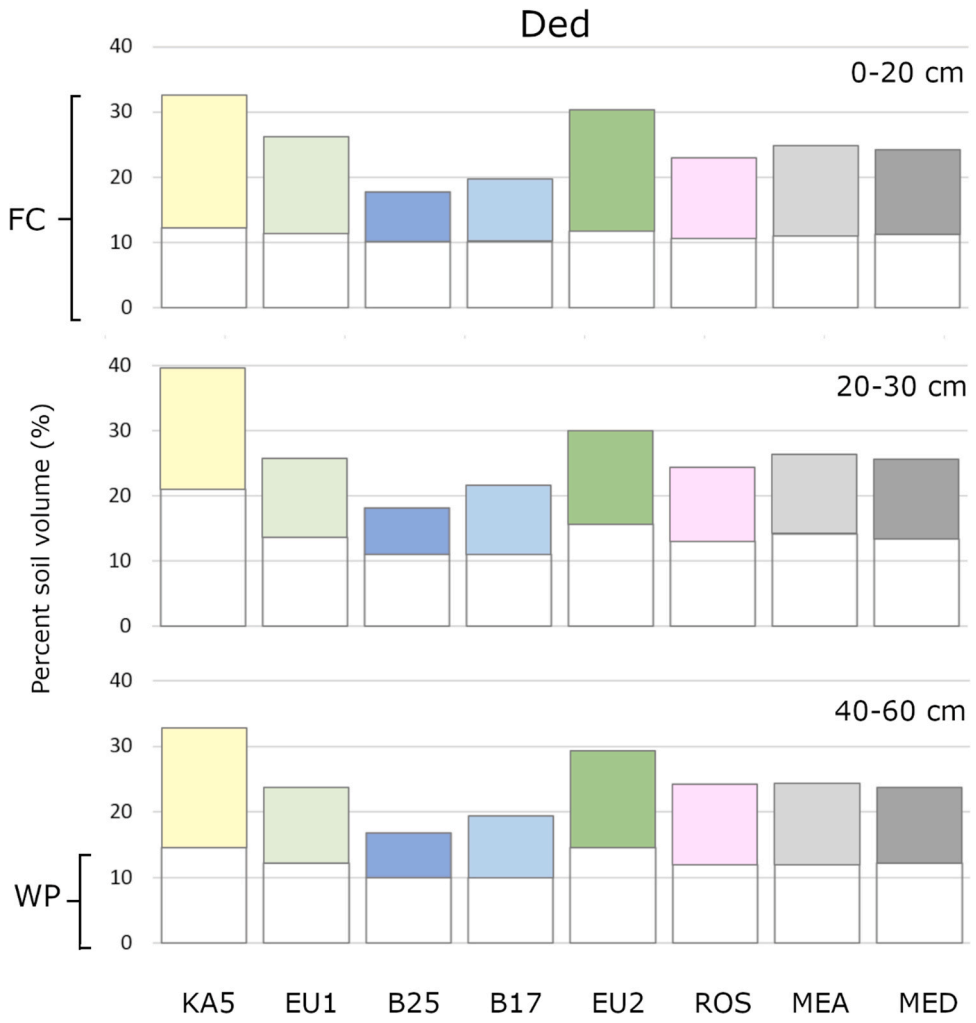

Fig. 5. Ded site average of field capacity (total bar height) and wilting point (white bars) at different soil depths predicted by each PTF (KA5, EU1, B25, B17, EU2 and ROS) and the PTF ensembles (MEA and MED). Color bars indicate soil available water capacity (AWC). (Colors were chosen only to enhance visualization).

At Ded, one of the sites with continuous time series of measured soil water content, regardless of the PTF used, HERMES simulations followed the seasonal patterns in soil water content (Figs. 11 and 12). The simulation shown corresponds to Plot 15, a soil profile with relatively low sand content (around 50 % at the upper 65 cm) and medium (16 % at 0–30 cm deep) to high (26 %, at 30–65 cm) clay. Some differences between modeled and measured soil water dynamics can also be observed: during the fall-winter months, when soils tend to reach higher values of soil water content, measurements oscillate around this water content value, whereas simulations, because of the way HERMES is programmed, does not exceed FC, giving the appearance of a straight line. This static behavior of the soil water content in the model during winter, influences the redistribution of water across the soil profile and consequently on groundwater recharge.

As observed at Boo, during the periods with high water content the measured values oscillate around simulated water contents from PTFs and PTF ensembles that estimated intermediate values of FC, such as MEA and MED. The sharp drop in the water content measured during the winter months of 2015–2016 can be related to a freezing event.

The relatively high errors of the simulations at site Due (MAE, Table 4) are evident when comparing the simulated with the measured dynamic soil water content (Fig. 13 and 14), where no single PTF closely matches the measured water content. Most simulated water content values are too high at 0–30 cm (Fig. 13) or too low at 30–60 cm (Fig. 14) respect to the measured water content. At 0–30 cm the measured soil water content abruptly decreased in January 2017, in clear contrast to the simulations. This strong drying out during the season can be due to lateral water drainage. As seen in previous cases, PTF-generated water content maxima seem consistent with their estimated FC values (KA5 and EU2 high FC, and ROS the lowest FC, Fig. 6).

3.3. Pedotransfer functions and yield simulation

The overall effect of PTFs on yield simulation did not show a definite trend across sites and years (Table 5). This means that no single PTF consistently showed low or high yield values in all cases. Nevertheless, KA5 produced often the highest yield value, and B25, the lowest. This suggests that there might be a direct impact of estimated AWC (and/or FC) and simulated yield, although not so clear for other PTFs that produced intermediate WRP values.

The highest mean CVs were observed at Boo (0.32 and 0.26, Table 6), indicating that the natural soil variability at the site might have an impact on the diversity of PTFs as WRPs estimators, and consequently, on the simulated yield. A one way ANOVA analysis, however, resulted in statistically significant yield differences only in 2021 ($F\ [8, 126] = 15.91$, $p = 4.8E\text{-}16$; Table 7) indicating that the high CV in 2020 is the result of a variability that had no clear pattern across PTFs, meaning that a given PTF did not have a consistent relationship respect to other PTFs across plots (compare the relationship between KA5 and other PTFs, for example, in 2020 and 2021 in Fig. 15). In 2021, when there was a significant effect of PTF choice on yield, the rank of simulated yield quantities (Table 5) closely follows the rank of WRPs (Fig. 3) that is,

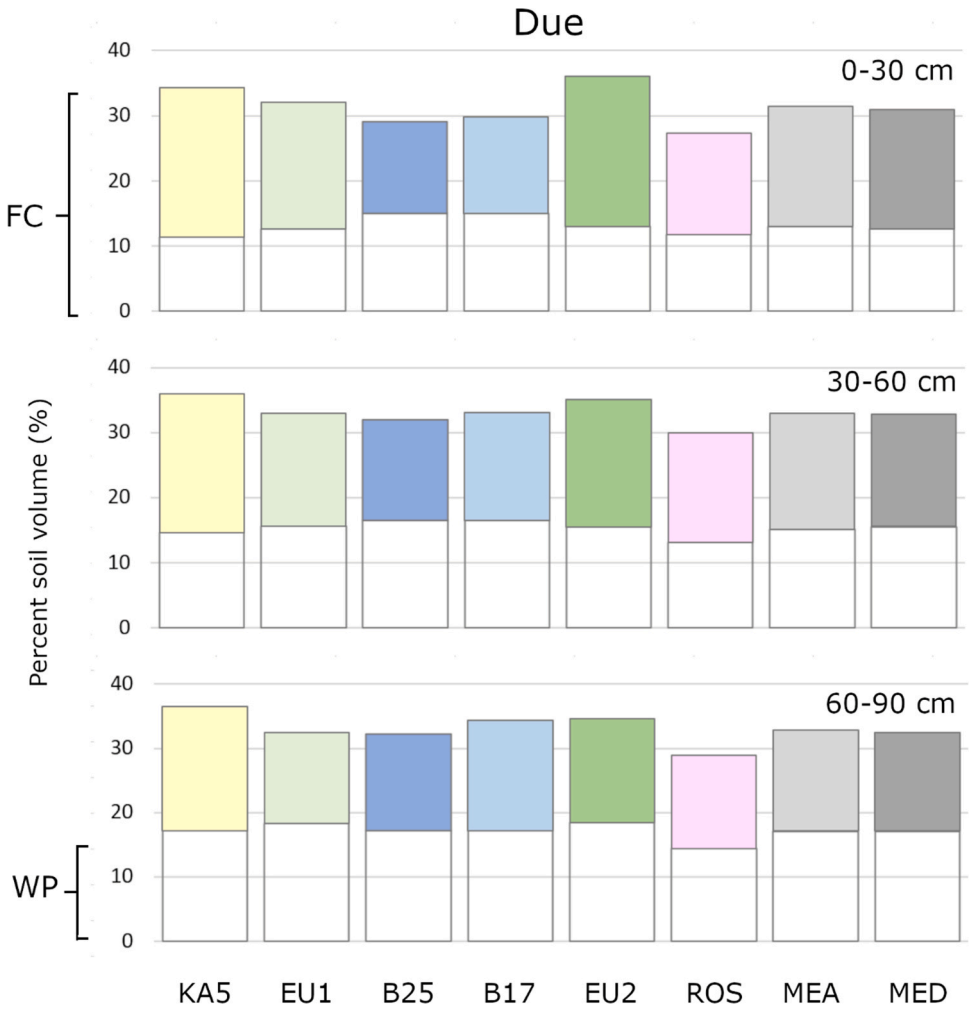

Fig. 6. Due site average of field capacity (total bar height) and wilting point (white bars) at different soil depths predicted by each PTF (KA5, EU1, B25, B17, EU2 and ROS) and the PTF ensembles (MEA and MED). Color bars indicate soil available water capacity (AWC). (Colors were chosen only to enhance visualization).

higher estimated FC corresponded to higher simulated yield.

At Ded, only OA 2018 showed a relatively high CV (0.26), one year of intermediate values (0.13), and two years with very low CV (0.01 and 0.05; Table 6). Despite the high CV values, however, in no case the ANOVA analyses indicated statistically significant differences (Table 7), although OA in 2018 (an extremely dry year), was almost significant ($F[8, 36] = 1.94$, $p = 0.08$; Table 7). In this case, as it was for the site Boo, simulated yield averages (Table 5, and some cases in Fig. 16) showed a ranking similar to the ranking of WRPs (Fig. 3). That is, KA5 high, the two EUs intermediate and B25, the lowest.

At Mar, in accordance with the relatively low CV values (0.06–0.09), none of the years showed a significant effect of the PTF choice (Table 7). The closest result to significant differences between yield simulation was CO 2020 with $F[8, 72] = 0.68$, and $p = 0.71$ (Table 7). Beyond these results, in 2020 and 2021 the ranking of yield from the PTFs (Table 5) corresponded to the ranking of the WRPs, suggesting, as in previous sites, that the estimated FC can have direct effect on simulated yield. It is also interesting to note that at plots where the simulated yield was relatively low (plots 1, 3, 6, 7 and 9, starting from the left on Fig. 17), the yield and FC varied together. However, this was not the case in plots with high simulated yield where PTFs such as B25 and B17 also produced high yields.

At Due, the site with the lowest overall CVs (0.03–0.08, Table 6), no significant effect of PTF choice on simulated yield was found. Additionally, and unlike the previous sites, the ranking of simulated yield at each plot (Fig. 18) seemed to follow an inverse order respect to FC, that is, PTFs with higher yield simulations (e.g. B25 and B27), had lower estimated FC values (Fig. 6). Although in 2020 no fertilizer was applied, plots 15, 16, 29, 30, 43 and 44, which had been fertilized in previous years showed a noticeable higher simulated yield than the control plots (numbers 23, 37 and 51). This also holds for the measured yield. Since control plots were spatially intercalated respect to the fertilized plots (no block effect possible), it can be presumed that in both the simulated and the measured yields, there could be a residual effect of previous years' fertilization.

Most of the variability in yield prediction from the PTFs occurred at sites with higher sand contents, raising the question of whether soil texture might have to do with differences in simulated yield. Since differences in yield often seemed to be a consequence of differences in WRPs, the deviation in FC estimates between contrasting PTFs (high vs. low FC-estimating PTFs) with respect to the soil sand contents provided some insights on the trends (Fig. 19). The pairs KA5-B25 and EU2-B17 were chosen to be displayed because KA5 and EU2 had the highest FC estimates, and B25 and B17, the lowest.

FC differences between KA5 and B25 seemed to have a relatively high value at around 50–60 % of sand (Fig. 19 A), whereas FC differences between EU2 and B17 had its maximum absolute value at around 80 % soil sand content (Fig. 19 B). To this respect, was the synthetic soil analysis particularly illustrative.

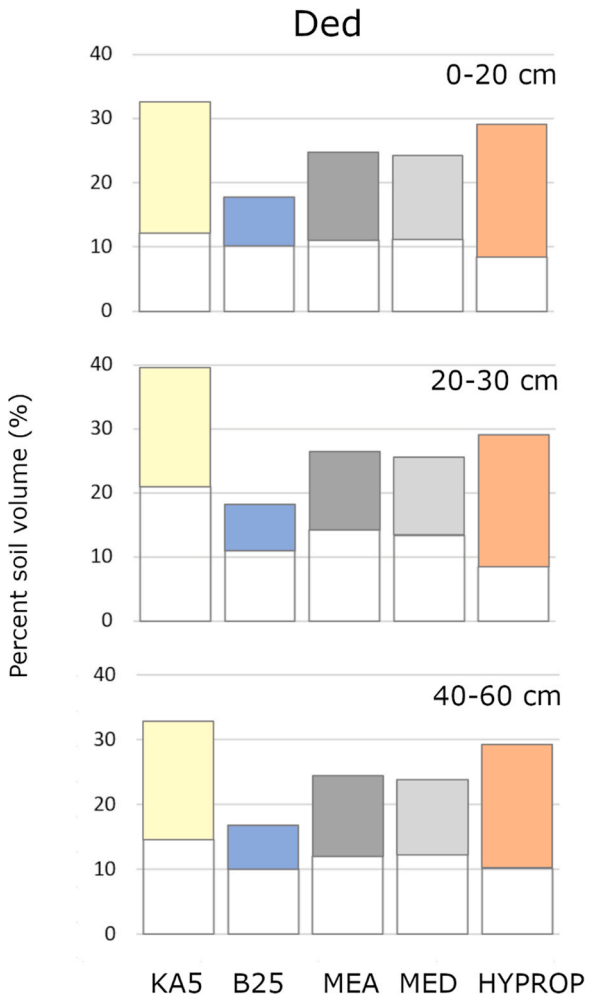

Fig. 7. Ded site average of field capacity (total bar height) and wilting point (white bars) at different soil depths predicted by some selected PTF (KA5, B25) and the PTF ensembles (MEA and MED) to compare with HYPROP estimates. Color bars indicate soil available water capacity (AWC). (colors were chosen only to enhance visualization).

3.4. Synthetic soil texture and PTFs

PTFs showed different WRP trends across the texture gradients of the synthetic soil database (Fig. 20). KA5 and EU2, for example, showed clear discontinuities in FC at around 75 % sand content (Fig. 20), which coincides with discontinuities in clay and silt percentages in the synthetic soil series (Fig. 2). Other discontinuities in KA5 are obviously related to the fact that KA5 is categorical by nature (Table 3). PTFs B25 and B17 did not present discontinuities, but changes in trend direction at 75 % and at about 90 % sand. Most of the vertical dispersion (small differences in FC values) of points belonging to the same PTF correspond to estimates at different depths in each soil profile.

As observed in some simulations of the experimental sites (Fig. 15, below; Fig. 16; and Fig. 17), in the synthetic soil simulations yields tended to be higher for simulations using PTFs that estimate higher FC or AWC. The higher yield obtained from the high FC estimating PTFs (KA5 and EU2) was consistently high (around 4000–3000 kg/ha) across most of the entire sand content gradient (Fig. 21, above). In 2021, KA5 and EU2 were also higher than the other two PTFs but to a variable degree across the sand content gradient (Fig. 21, below).

Within each PTF, yield tended to decrease with increasing soil sand content (Fig. 21). In the case of B25 and B17, the decrease was more gradual and across the entire sand scale, whereas for KA5 and EU2 the decrease happened mostly at higher sand contents. This suggests that PTFs that estimate less water availability in soils tend to be more sensitive to smaller decreases in soil retention capacity (increasing sand) when estimating plant productivity.

Higher yield differences between PTFs seemed to occur at around 60 and 90 % sand content in 2020 (Fig. 21, above) and around 70 % in 2021 (Fig. 21, below). These three critical percent values seem to coincide with discontinuities (in the case of KA5 and EU2) or changes in direction (in the case of B25 and B17) in the FC-sand content relationships (Fig. 20). This implies that the impact of the choice of PTF on yield is a function of how close the soil texture values are to these points at which FC discontinuities occur. This might explain the fact that the highest variation in yield between PTFs (Table 6) occurred at Boo and Ded: soils from both sites included two or three of the sand percent critical values (Fig. 20, upper bars).

4. Discussion

One of the main problems when trying to find the most accurate PTF is the availability of reference values, that is, direct measurements of soil water retention parameters. On the one hand, these measurements are difficult or impractical to perform (Bagnall et al., 2022), and on the other hand, one of the main parameters, FC, is defined differently in different regions (Batjes, 1996). Even the definition of what constitutes sand, silt or clay in terms of particle size can vary between countries (Burt, 1996; Eckelmann et al., 2005; Pachepsky and van Genuchten, 2011).

Bulk density requires special attention. With the increasing need in estimating long term soil carbon (Xu et al., 2016; Walter et al., 2016) and in maintaining soil health (Panagos et al., 2024; Chen et al., 2024) this soil parameter has gained significance (Ramcharan et al., 2017). The frequent lack of information on bulk density is related to the fact that direct methods of measuring it are expensive and labor intensive (Al-Shammary et al., 2018; Panagos, 2024; Walter et al., 2016), especially at deeper layers (Xu et al., 2016). Therefore, it is not coincidence that the two sites at which bulk density measurements were available were part of long-term studies. Probably a reflection of the difficulties in determining bulk density is the fact that not all PTFs tested in this study require bulk density for their calculation. In the case of EU1 and EU2, which have several algorithms to choose from, less than half of these options include bulk density in their formulations. Given the relationship between bulk density and soil depth (Panagos et al., 2024) the absence of the former in the algorithms might be compensated by the inclusion of soil depth or position in the soil profile (top- or subsoil) in all EU2 and most EU1 formulations.

4.1. PTFs and soil water

Beyond the exact determination of the FC value for a given soil, FC is by convention the amount of water that remains after the water saturated soil profile has drained by gravity; a process that may take between some hours and a day (Evett et al., 2019). In colder or temperate climates during the months of low temperature and plant activity, soil water contents exceeding FC quickly drains and soil water contents tend to remain around FC levels, until the beginning of the growing season, when water starts to be utilized by plants or to evaporate due to the increasing temperatures. The resulting pattern of higher values in fall/winter and lower in spring/summer can be seen in the measured values of Figs. 11 and 12.

The strong influence of FC in water simulations is also present in HERMES, because this model does not allow water saturation to persist more than one day. This explains the tendency to form high plateaus close to FC in the simulations as seen on Figs. 9–13 during the fall and winter months. As a consequence of this dynamics, substantial differences in FC estimates from the different PTFs, would produce also large differences in overall available soil water predictions, in a fairly direct relationship, i.e., higher FC values corresponding to more available

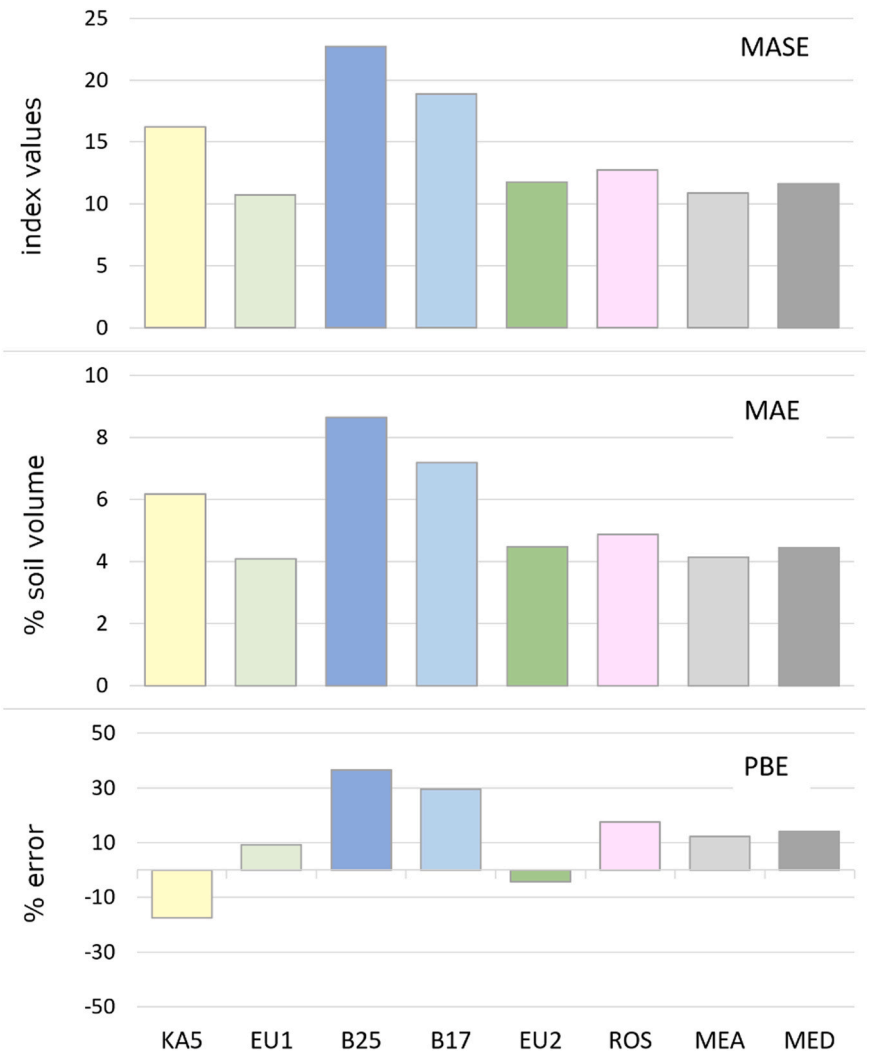

Fig. 8. Mean absolute scaled error (MASE), mean absolute error (MAE), and percentage bias error (PBE) of the simulated soil water dynamics compared to measured values at Ded). (Colors were chosen only to enhance visualization).

water (provided that differences in simulated WP are less significant, as seen in Fig. 3, for example).

We did not have any evidence that the plateaus observed in measured water contents corresponded to the "real" or effective FC of that soil; however, at Ded (Fig. 11, 9 and 12) the measured soil water content maxima formed a jagged, horizontal line at around the same value in all seasons, suggesting that this could correspond to the FC parameter. At Due (Figs. 13 and 14) a maximum line was not so clearly present, and high peak fluctuations varied in values of around 5–10 % from season to season, making it difficult to draw any conclusion about the most likely soil parameter values. The reasons for these fluctuations are not clear. Freezing events in winter and cracking of drying soil in summer, and tillage practices (Liebhard et al., 2022) are possible reasons. Additionally, inaccuracies in the measurements themselves cannot be ruled out.

If, nevertheless, we accept the observations at Ded as a valid criterium for determining the magnitude of FC, then the water content at FC is accurately predicted if the maximum values of simulated water contents match with those of the observed ones.

At Ded, PTFs that estimated intermediate FC values, like RAW and EU1, and the PTF ensemble MEA (Fig. 5) produced the most accurate simulations (Table 4), indicating that the actual FC of the site must be at around 25 %. At Boo, also the intermediate FC estimates (PTFs RAW, MEA and MED) showed less error (Table 4), but in this case a mean FC of 15–17 % would be the most likely value. In the case of Mar, in contrast to the previous sites, the most accurate PTFs were the ones estimating the lowest FC values, B25, B17 and ROS. However, these estimates correspond to FC averages ranging from 8 % to 14 %, placing Mar close to Boo in terms of soil parameters magnitudes. Therefore, it follows that two PTFs could work differently at two sites even though both sites have similar WRP values.

Alternatively, it could be that in the concrete case of Boo versus Mar, the slight differences in the estimated (most likely) FC values (in the order of 1–7 %) are enough to increase the chances of one PTF with respect to the other. In this case, the sensitivity of PTFs to slight changes in texture shown in Fig. 20 becomes particularly relevant.

In summary, at Boo, Ded and Mar sites, KA5 and EU2 (and also HYPROP at Ded, Fig. 7) clearly overestimated FC values and the amount of water. MEA and MED PTF ensembles produced accurate results in sites like Boo or Due (Table 4), where soil water content was more closely simulated by FC of intermediate magnitude (Figs. 3 and 5) such as ROS, due to the fact that with the mean and the median the extremes tend to cancel each other. In these cases, an advantage of the PTF ensembles is that analysts do not need to make elaborate decisions on which PTF to use in each case.

Table 4
Mean absolute error (MAE in % vol) and percent bias error (PBE in % of measured values) of simulated versus measured soil water content values by sites. KA5, EU1, B25, B17, EU2 and ROS: pedotransfer functions used for the simulations (see Table 3). Blue background shows the three best performers (lowest MAE) at each site.

Site		KA5	EU1	B25	B17	EU2	ROS	MEA	MED
Boo	MAE	5.02	3.08	3.14	2.94	5.09	3.35	2.49	2.50
	PBE	-37.18	-19.80	24.89	19.33	-34.14	-3.35	-11.93	-10.53
Mar	MAE	8.15	5.15	2.47	2.33	6.73	2.33	3.84	3.57
	PBE	-93.00	-58.84	19.56	13.95	-75.67	-20.52	-43.04	-40.36
Ded	MAE	6.18	4.09	8.65	7.19	4.48	4.86	4.14	4.43
	PBE	-17.44	9.29	36.57	29.69	-4.44	17.60	12.30	14.16
Due	MAE	6.76	8.45	7.70	7.58	8.03	9.11	8.06	7.84
	PBE	6.28	14.67	17.84	14.27	6.47	26.50	15.10	16.01
Average	MAE	6.80	5.25	5.48	5.01	6.27	4.99	4.73	4.64
	PBE	-35.34	-13.67	24.72	19.31	-26.95	5.06	-6.89	-5.18

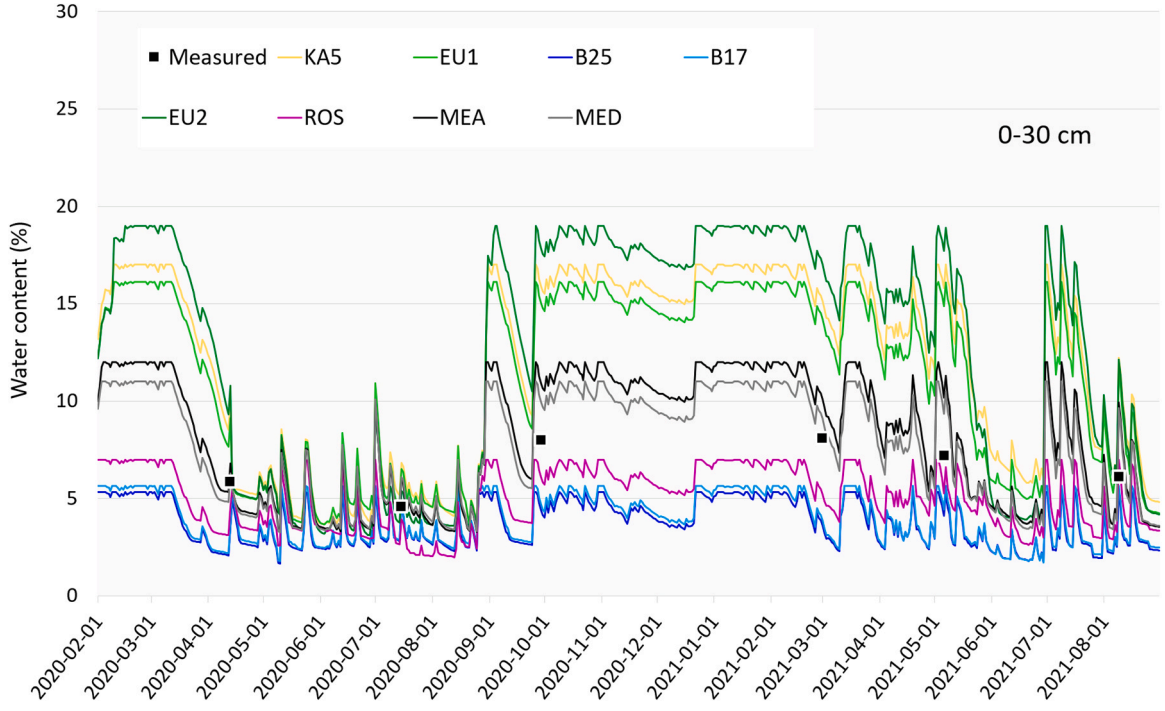

Fig. 9. Soil water content simulations at the Boo site (0–30 cm depth) using all pedotransfer functions (PTFs, Table 3) compared with measured data.

4.2. PTFs and yield

Regarding the question of whether PTFs can have a big impact on yield simulation, the results of the synthetic soil model runs indicate that impacts can manifest themselves in two ways:

a) in a constant manner across most of the soil sand content as observed in 2020 (compare KA5 with B17 in Fig. 21, above), and b) in a variable way around specific soil sand percent contents (KA5 and EU2 in Fig. 21, below), most likely related to points at which PTFs present discontinuities in the WRPs estimates as a result of transition zones in the texture continuum.

In the first case, it is possible that at specific growth conditions related to crop properties, for example, drought tolerance, and the season's weather, for instance, enough precipitation, makes the amount of AWC becoming particularly relevant. Then, PTFs that tend to estimate higher FC values simulate higher yields independently of the texture value (that is, within the range of the synthetic texture in this study). It might be tempting to try to verify this presumption with the results of the yield simulations of the 2020 experiments at the site of Boo (same year, same crop and a wide range of soil sand content). However, in this case, in most of the plots B25 and B17 PTFs produced higher yields than KA5 and EU2 (Fig. 15, above). This is because real soils do not have

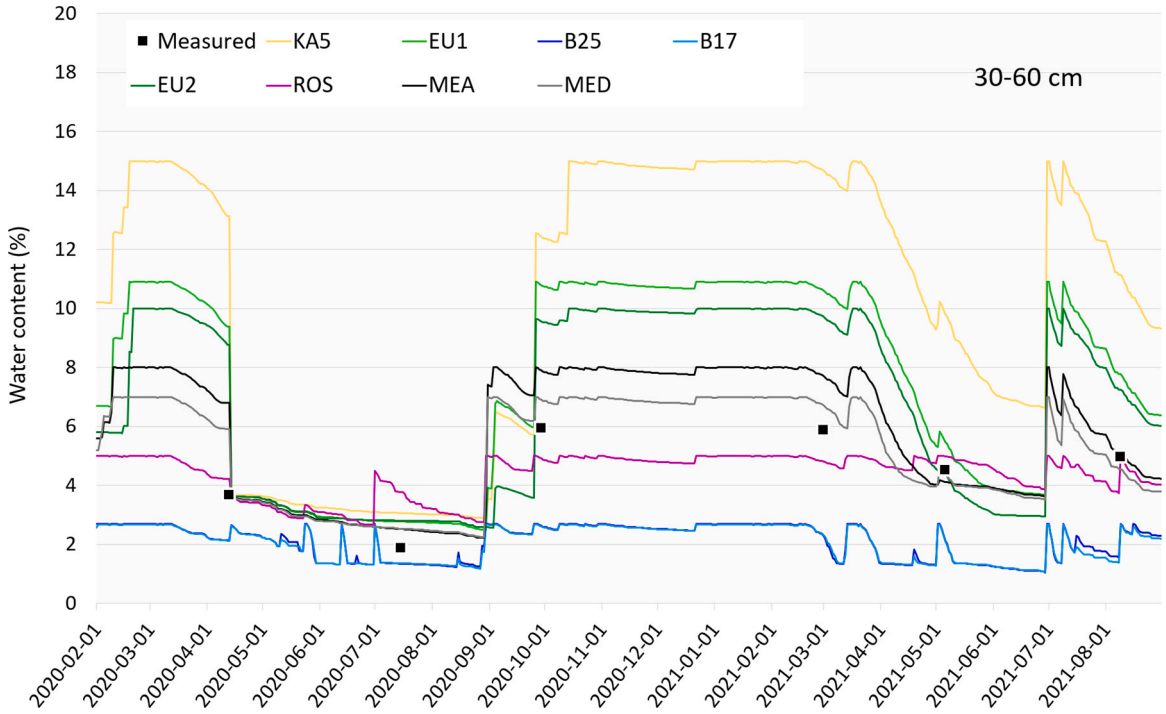

Fig. 10. Soil water content simulations at the Boo site (30–60 cm depth) using all pedotransfer functions (PTFs, Table 3) compared with measured data.

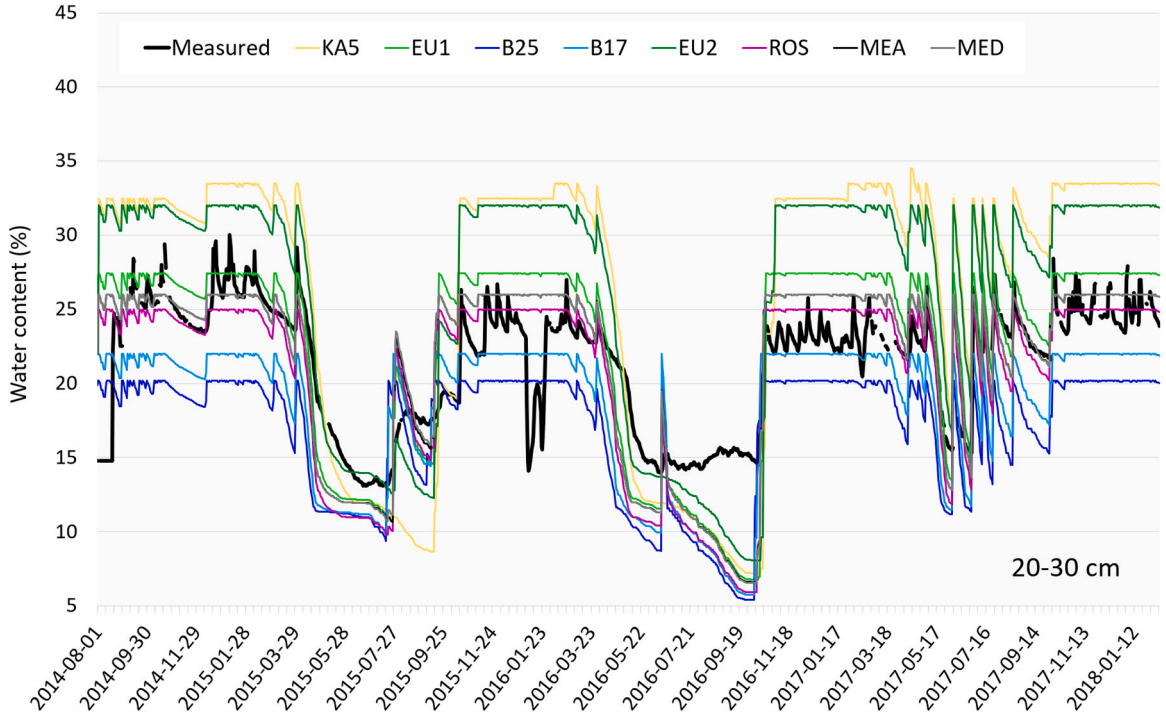

Fig. 11. Soil water content simulations at the Ded site (20–30 cm depth) using all pedotransfer functions (PTFs, Table 3) compared with measured data.

uniform texture values across the soil profile, whereas profile uniformity was a premise in the generation of the synthetic soil database.

The second type of impact may be related, at least in part, to the difficulty of establishing a completely gradual synthetic database. Even when sand content followed a smooth scale of 2 % steps, non-gradual changes in silt and/or sand may produce discontinuities in the resulting WRPs. For example, at the 90 % sand content, where both the trends of FC and yield appeared to show a clear discontinuity (Figs. 20 and 21, respectively), it coincided with a relatively abrupt increase in clay and a decrease in silt in the synthetic soil set (Fig. 2). These changes, although of few percentual points, seemed to have been high enough to affect the graduality of the FC estimates. Similarly, at 75 % sand content, where another FC and yield jump appeared (Fig. 19 and Fig. 20, respectively) there was another inflexion point in both clay and silt percentages (Fig. 2). The reasons for the relative impact of texture on the yield at varying conditions could be better understood with a sensitivity

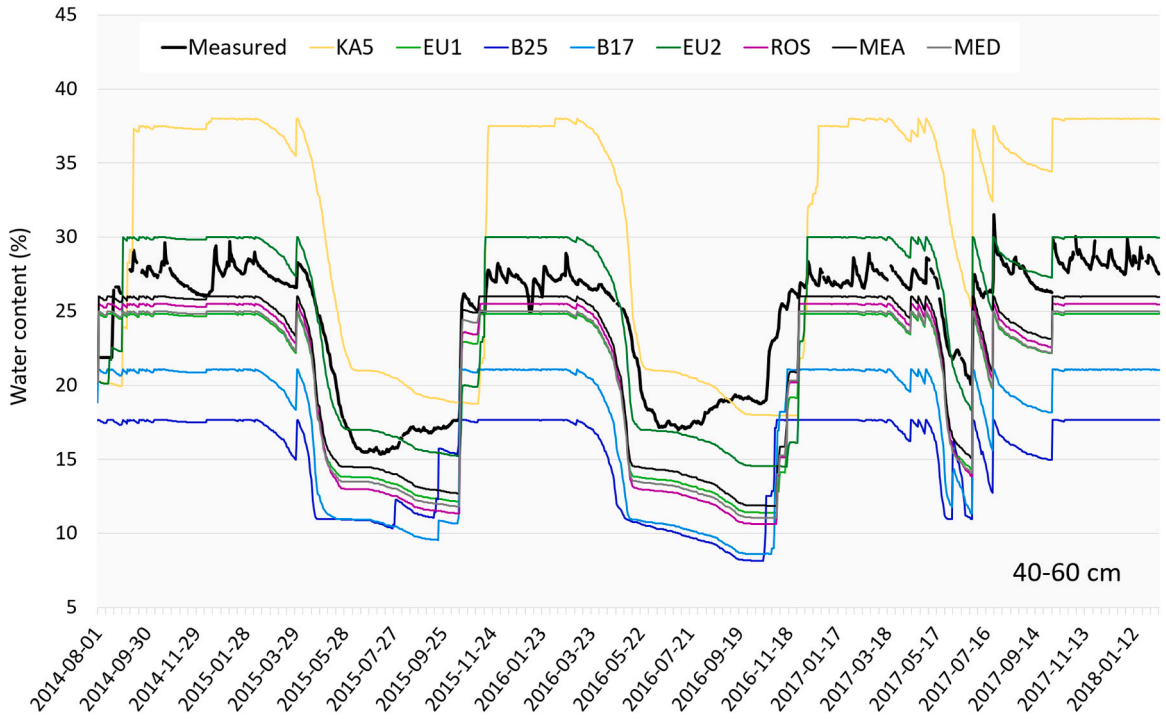

Fig. 12. Soil water content simulations at the Ded site (40–60 cm depth) using all pedotransfer functions (PTFs, Table 3) compared with measured data.

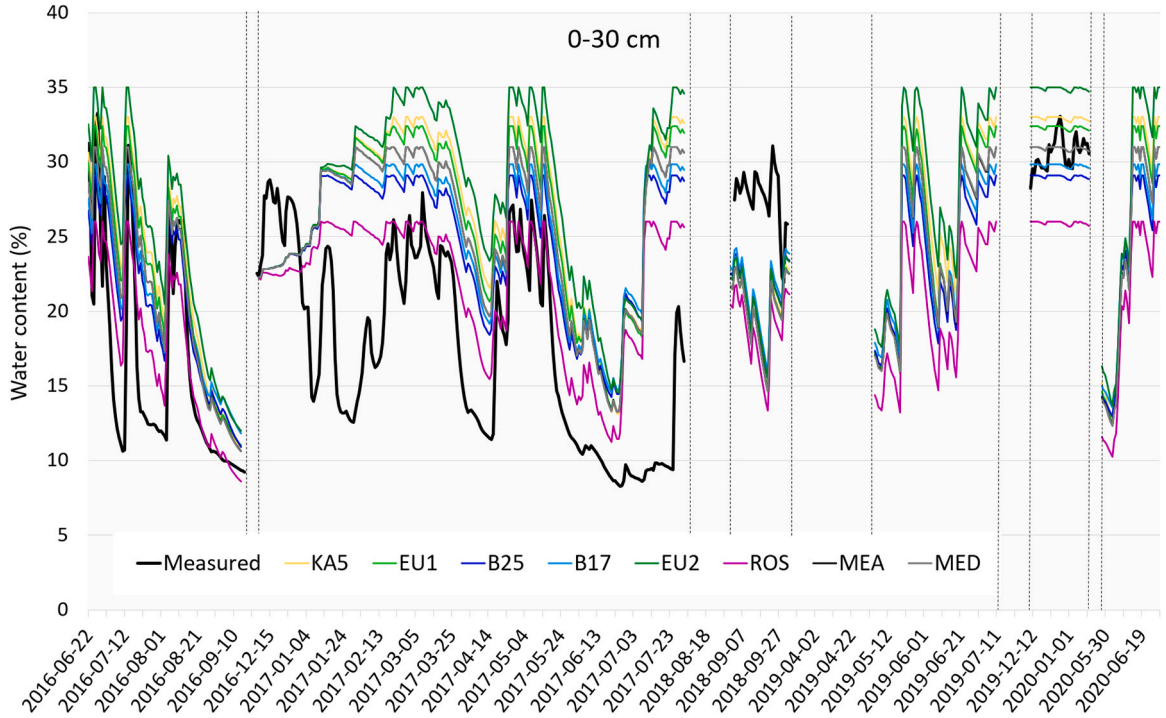

Fig. 13. Soil water content simulations at the Due site (0–30 cm depth) using all pedotransfer functions (PTFs, Table 3) compared with measured data. Vertical lines indicate discontinuities in the records.

analysis.

Non-linearity in the texture-WRP relationship can be also related to the definition of what constitutes sand, silt and clay. The German publication Soil Survey Guide (Eckelmann et al., 2005) on which the KA5 method is based, considers that the "sand" soil type (abbreviated "ss") should be actually separated in three subtypes according to the proportions of fine, medium and coarse sand, when it comes to characterize in more detail the WRPs. According to this guide, FC values can vary up to 6 % between soils with predominantly coarse sand and soils with predominantly fine sand. Besides the fact that there could be particle size subtypes at any other soil type, these subtypes could potentially create complex interactions in different combinations of clay, sand and silt. PTFs then may differ in the way they capture these complex interactions.

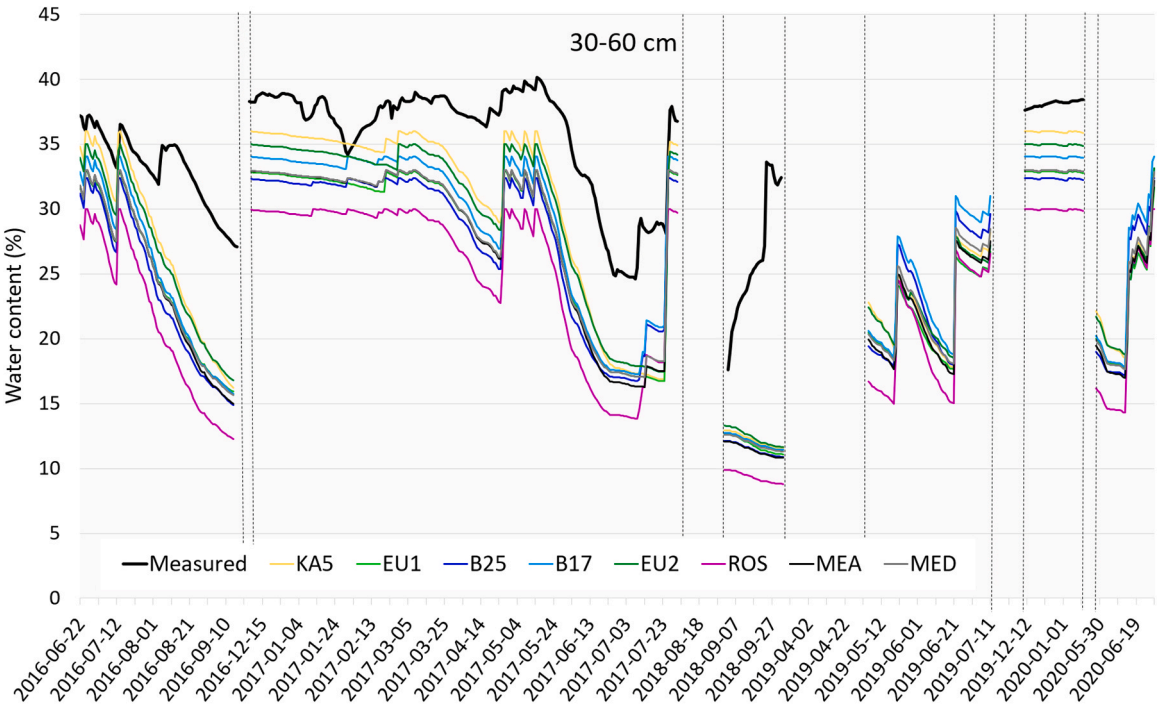

Fig. 14. Soil water content simulations at the Due site (30–60 cm depth) using all pedotransfer functions (PTFs, Table 3) compared with measured data. Vertical lines indicate discontinuities in the records.

Table 5
Simulated and measured yield (t/ha) with all the pedotransfer functions (PTF). In parentheses: number of SUs (plots). Yr: year. CO: corn, WR: winter rye, WW: winter wheat, OA: oat, SW: spring wheat. KA5, EU1, B25, B17, EU2, ROS, MEA and MED: pedotransfer functions used in the simulations (see Table 3). Avg: average. SD: standard deviation. Blue and red cells: highest and lowest average at each row, respectively.

Site	Crop	Yr	**Simulated yield** (average of all plots per year)							**Measured yield**
			KA5	EU1	B25	B17	EU2	ROS	MEA	MED	Avg (SD)
Boo	CO	20	7.6	9.3	8.6	9.3	7.7	6.3	6.9	6.9	9.4 (3.2)
(15)	WR	21	8.3	6.6	4.5	4.7	8.3	5.3	5.9	5.8	6.4 (1.7)
Ded	WW	15	8.9	7.1	6.8	6.9	7.8	7.3	7.2	7.1	9.4 (1.7)
(5)	WW	16	7.1	6.6	6.2	6.6	6.7	6.7	6.7	6.7	7.5 (0.9)
	WR	17	9.3	9.3	9.0	9.3	9.3	9.3	9.3	9.3	8.7 (1.9)
	OA	18	5.3	3.3	2.2	2.6	4.3	3.1	3.3	3.2	3.1 (0.7)
Mar	WR	19	7.6	7.4	8.2	8.1	7.5	7.9	7.3	7.4	6.2 (0.5)
(9)	CO	20	15.7	15.1	14.0	14.0	15.6	13.9	14.3	14.7	15.4 (1.8)
	WR	21	8.8	8.0	7.4	7.4	8.6	7.5	7.8	7.7	7.2 (1.6)
Due	CO	16	15.7	14.9	14.6	15.2	14.6	14.9	15.4	15.2	12.7 (4.8)
(9)	WW	17	8.7	8.5	8.5	8.9	8.7	8.6	9.0	9.0	7.6 (3.6)
	CO	18	10.8	10.3	10.2	10.6	10.3	10.3	10.6	10.6	11.2 (2.6)
	WW	19	8.7	8.6	8.6	8.8	8.6	8.6	8.8	8.8	9.4 (4.3)
	SW	20	3.2	3.6	3.9	3.9	3.1	3.9	3.7	3.8	5.0 (0.6)

Table 6
Coefficient of variation (CV) of the PTF-based yield (t/ha) averaged by site and year. n: number of plots (Sus). CO: corn, WR: winter rye, WW: winter wheat, OA: oat, SW: spring wheat.

Site	Crop	Year	CV
Boo	CO	2020	0.32
(n = 15)	WR	2021	0.26
Ded	WW	2015	0.13
(n = 5)	WW	2016	0.05
	WR	2017	0.01
	OA	2018	0.26
Mar	WR	2019	0.06
(n = 9)	CO	2020	0.09
	WR	2021	0.09
Due	CO	2016	0.04
(n = 9)	WW	2017	0.04
	CO	2018	0.05
	WW	2019	0.03
	SW	2020	0.08

Table 7
ANOVA results for sites and years relatively closer to significance. df btw and df wthn: degrees of freedom between and within groups respectively; F: F-statistic; P-value: significance level; and F-crit: critical F value.

Site Year	df btw	df wthn	F	P-value	F crit
Boo 2020	8	126	1.39	0.21	2.01
Boo 2021	8	126	15.91	4.8 e−16	2.01
Ded 2015	8	36	0.15	1.00	2.21
Ded 2018	8	36	1.94	0.08	2.21
Mar 2020	8	72	0.68	0.71	2.07

Beyond the magnitude of the impact of PTFs on yield, we observed some trends in the relationship between simulated yield and PTFs. As it was for soil water simulations, yield simulations with the different PTFs often showed a correlation with their estimated FCs. This means that, according to the model's dynamic principles, high estimated FC values often corresponded to higher water contents and higher yields.

In the field, more water may have a direct effect on yield because of the higher water availability, and indirectly, it could be related to lower losses of nitrogen by leaching. In the case of Due, although there was some consistency in the FC-soil water correlation, no correspondence between FC and simulated yield was evident. This might have to do with the fact that in soils with less sand content soil water is a less important limiting factor, given the differences in critical soil water thresholds between fine and coarse soils (Wankmüller et al., 2024).

The ranking of simulated yield at Due did not resemble the ranking of FC or soil water content. However, the yield ranking at Due shares some features with the simulated yield ranking in the productive plots (plots 2, 4, 5 and 8, starting from the left on Fig. 17) at Mar. Boo also showed such an inversion in yield with respect to FC for most plots in 2020 (corn), but not in 2021 (winter rye) (Fig. 15). Corn was also grown at Mar in 2020. We could speculate that at certain conditions, for example

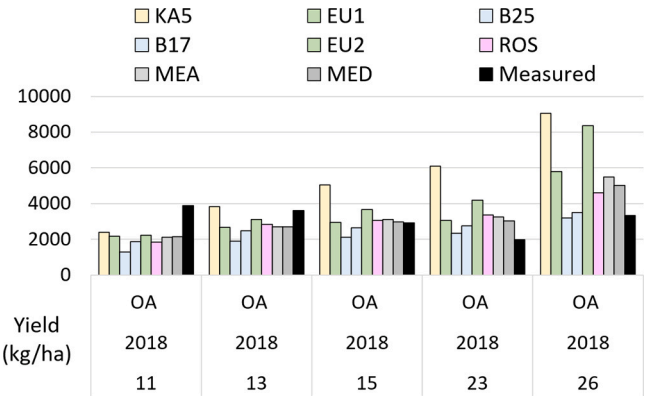

Fig. 16. Predicted yield for each PTF and measured yield at Ded in 2018. Each block of bars represents one plot. X axis: first row is crop (Table 6); second, year; and numbers 11–26 are plot numbers.

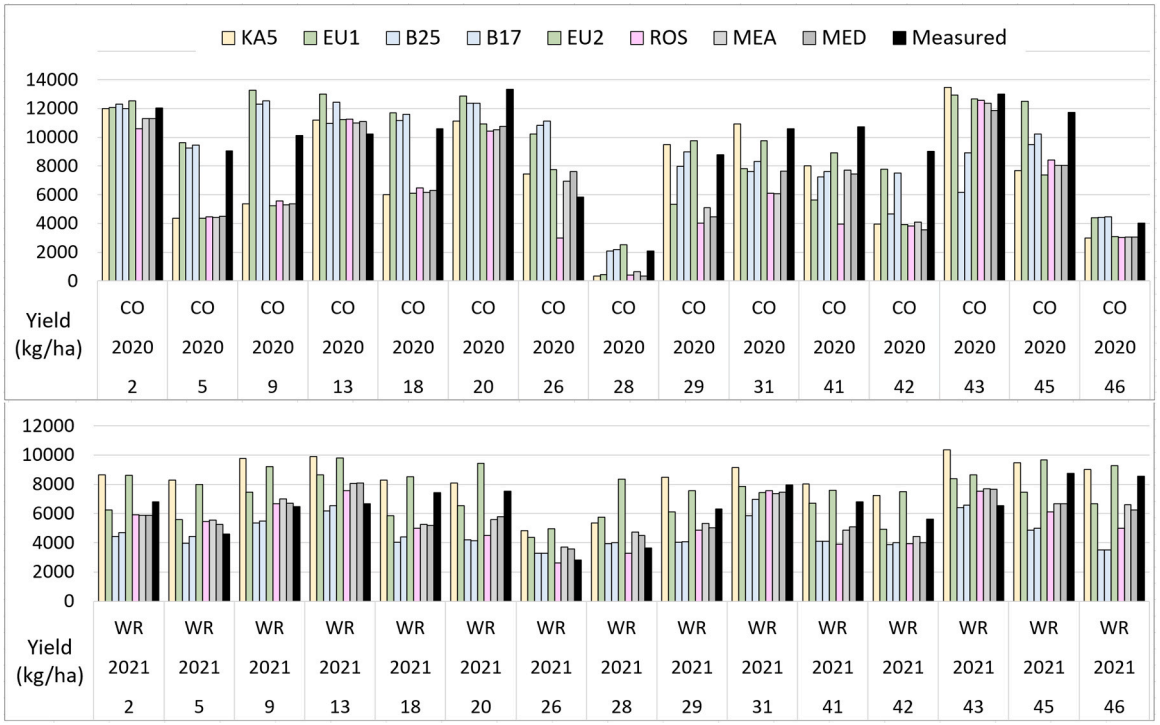

Fig. 15. Predicted yield for each PTF and measured yield at Boo in 2020 and 2021. Each block of bars represents one plot. X axis: first row is crop (Table 6); second, year; and numbers 2–46 are plot numbers.

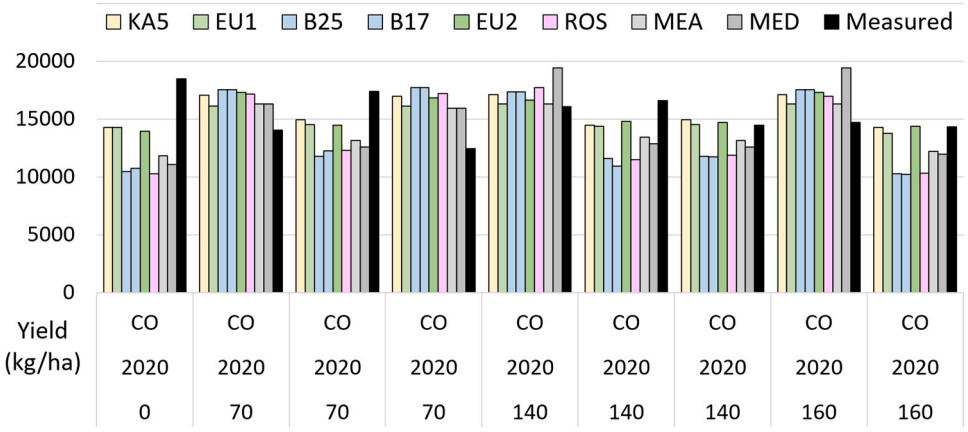

Fig. 17. Predicted yield for each PTF and measured yield at Mar in 2020. Each block of bars represents one plot. X axis: first row is crop (Table 6); second, year; and numbers 0–160 are fertilization amounts in kg N/ha.

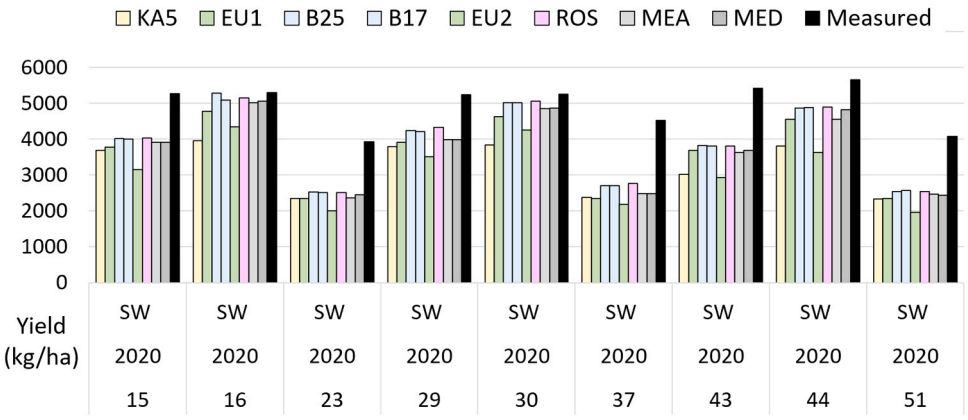

Fig. 18. Predicted yield for each PTF and measured yield at Due in 2020. Each block of bars represents one plot. X axis: first row is crop (Table 6); second, year; and numbers 15–51 are plot numbers.

when water availability is not a limiting factor, or when specific crops (e.g. with different root distribution patterns) are grown, PTFs that produce low FC estimates and lower soil water contents, could nevertheless result in high yield simulations. Groh et al. (2020) showed that models based on relatively simple representations of soil structure can fail to appropriately account for natural soil variability and its consequent effects on crop processes and outputs.

Another reason for the apparent inverse relationship between FC and simulated yield could be that PTFs like KA5 and EU2 that estimated relatively high FC values, end up in relatively small values of air capacity as the difference between FC and the total available soil pore space (PS) can be too small. In this study, the differences between PS (data not shown) and FC could attain values of less than 5 % at Due, which might be too low to allow for an optimal plant growth when soil moisture is at full FC due to critical soil air content. In HERMES the critical threshold for air content triggering oxygen stress is mostly at 8 % of soil volume.

Finally, it should be underlined that even though the findings of this study are restricted to the application of a single simulation model, in light of the significant departures in estimating WRPs from the different PTFs, analogous effects could be expected for other models using soil water capacity-based (tip-bucket type) approaches.

5. Conclusions

In conclusion, the choice of pedotransfer functions (PTF) resulted in most cases in measurable differences in soil water content dynamics, often showing a direct relationship between field capacity (FC) and water content magnitudes, indicating that, for models that use a capacity approach, the accurate estimate of the soil water content at FC is crucial in the choice of PTF.

Differences in soil water content generated by the PTFs were more evident at periods of full FC or soil water saturation. This might be the reason for the relatively tight relationship between the estimated FC and water dynamics simulations.

The PTF ensembles produced relatively accurate soil water dynamics results in cases where some of the PTFs chosen produced too low and others too high WRP simulation values. In these cases, results suggest that ensembles simplify the analyst's decision on which PTF to use in each case

The KA5, a traditional method to estimate WRPs, seems to have a tendency to overestimate FC, and consequently, soil water content in sandy soils. With this method, a similar trend could be observed in clayey soils at Due, but this overestimation seemed less significant.

Under certain conditions, PTFs producing higher estimated FCs also resulted in higher yield, suggesting that the HERMES model yield simulation can be sensitive to soil water availability. Also, the PTFs tested in this study showed an increasing variability in WRP estimation and yield simulation at specific points in the sand percent continuum of the synthetic soil database, where non-gradual, but relatively small changes in silt and/or sand content occurred. This means that different PTFs have different degrees of sensitivity even at small changes in particle size distribution.

And finally, the importance of the soil water retention properties for simulating and predicting crop yield suggests the need for extending and

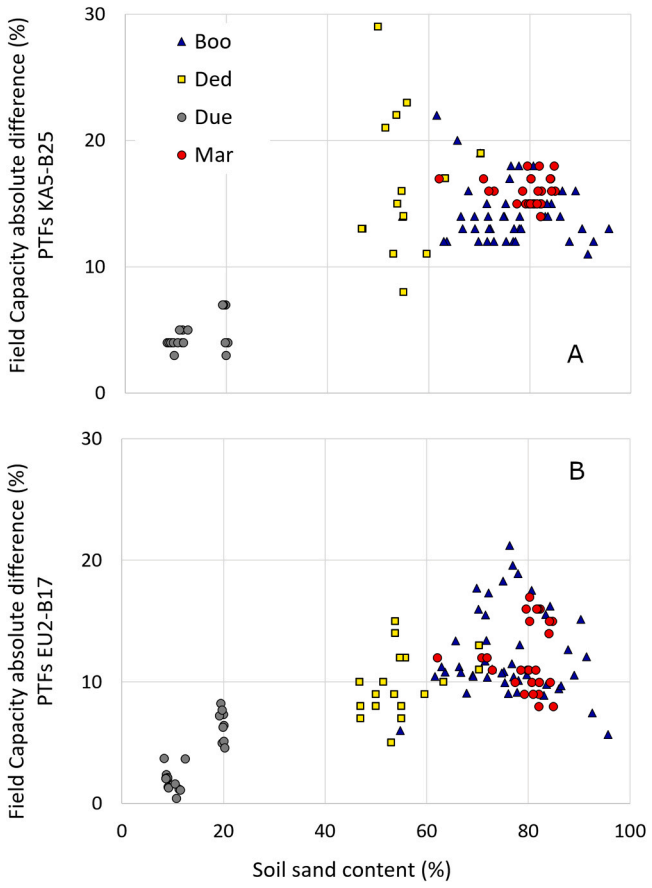

Fig. 19. Absolute differences in field capacity estimations between PTFs in relation to the sand content of the soils across all sites. A: KA5 minus B25, and B: EU2 minus B17. See PTF definitions in Table 3.

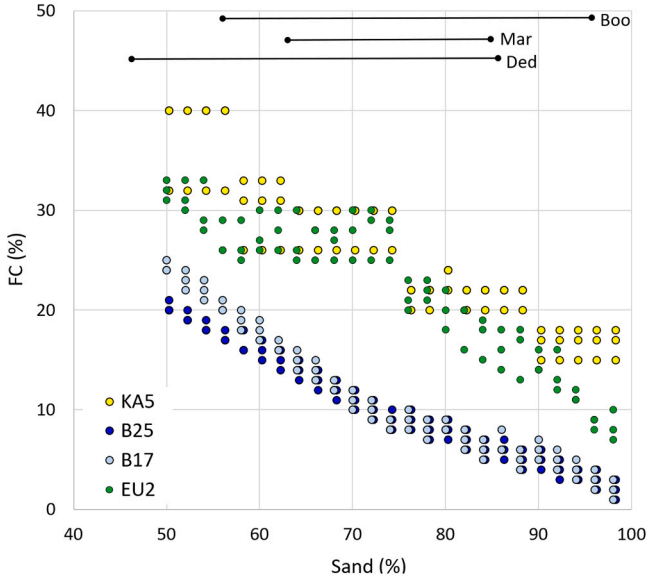

Fig. 20. Relationship between soil sand content and field capacity (FC) as estimated by the pedotransfer functions KA5, B25, B17 and EU2. Segments labeled Boo, Mar and Ded indicate the actual sand content range at each of these sites. Some points have been slightly horizontally displaced for visibility.

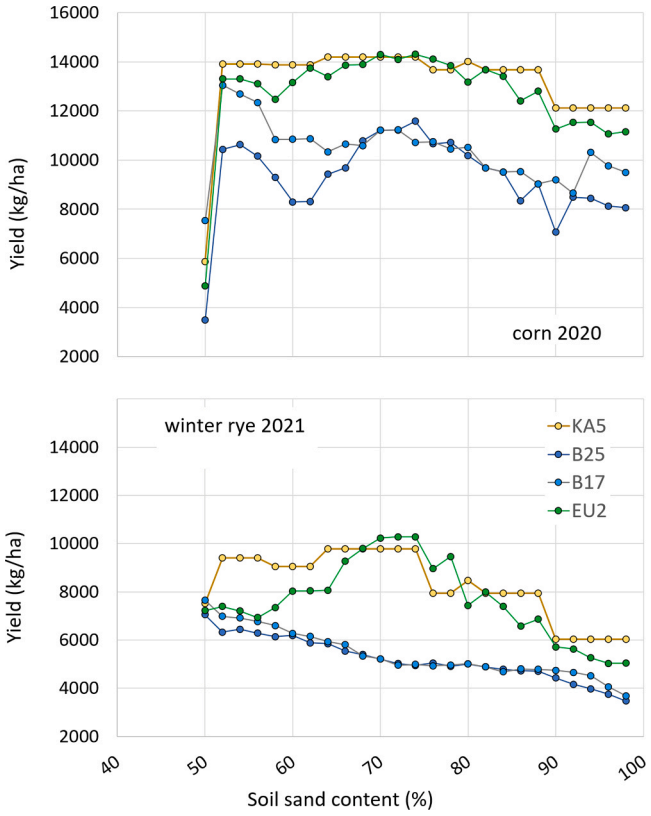

Fig. 21. Simulated yield with the synthetic soils at Boo for corn (above) and winter rye (below), respect to the sand content of the soils, for PTFs with high FC estimates (KA5 and EU2) and with low FC (B25 and B17).

improving the soil databases.

CRediT authorship contribution statement

Robin Gebbers: Writing – review & editing, Validation, Methodology. **Jannis Groh:** Writing – review & editing, Validation, Methodology, Investigation, Funding acquisition, Data curation. **K.-Christian Kersebaum:** Writing – review & editing, Methodology, Funding acquisition, Conceptualization. **Kurt Heil:** Writing – review & editing, Investigation, Data curation. **Horst H. Gerke:** Writing – review & editing, Validation, Investigation. **Pablo Rosso:** Writing – review & editing, Writing – original draft, Validation, Methodology, Investigation, Formal analysis, Conceptualization.

Declaration of Competing Interest

The authors declare the following financial interests/personal relationships which may be considered as potential competing interests: Pablo Rosso reports financial support was provided by Federal Ministry of Education and Research Berlin Office. Jannis Groh reports financial support was provided by Helmholtz Association of German Research Centres Berlin Office. K–Christian Kersebaum reports financial support was provided by AdAgrif. If there are other authors, they declare that they have no known competing financial interests or personal relationships that could have appeared to influence the work reported in this paper.

Acknowledgments

This work was supported by the German Federal Ministry of Education and Research (BMBF), Project I4S (http://www.bonares.de/i4s/; grant Number 031B1069B), which is part of the BonaRes program.

Jannis Groh is funded by the Deutsche Forschungsgemeinschaft (DFG, German Research Foundation; project no. 460817082). We also acknowledge the support of TERENO and SOILCan, which were funded by the Helmholtz Association (HGF) and the Federal Ministry of Education and Research (BMBF). K.-C. Kersebaum has received additional support from AdAgriF - Advanced methods of greenhouse gases emission reduction and sequestration in agriculture and forest landscape for climate change mitigation (CZ.02.01.01/00/22_008/0004635).

Appendix A. Pedotransfer functions formulas

EU PTF v.1

$$\theta PS = 0.6819 - 0.06480 \bullet (1/(OC+1)) - 0.11900 * BD^2 + 0.001489 * Cl + 0.0008031 * Si + 0.02321 * (1/(OC+1)) * \mathrm{BD}^2 - 0.00002315 * Si * Cl - 0.0001197 * Si * BD^2 - 0.0001068 * Cl * BD^2 \quad (A.1)$$

$$FC = 0.2449 - 0.1887 * (1/(OC+1)) + 0.004527 * Cl + 0.001535 * Si + 0.001442 * Si * (1/(OC+1)) - 0.00005110 * Si * Cl + 0.0008676 * Cl * (1/(OC+1)) \quad (A.2)$$

$$\theta WP = 0.09878 + 0.002127 * Cl - 0.0008366 * Si - 0.07670 * (1/(OC+1)) + 0.00003853 * Si * Cl + 0.002330 * Cl * (1/(OC+1)) + 0.0009498 * Si * (1/(OC+1)) \quad (A.3)$$

Batjes FC@2.5 pF:

$$\theta PS = 0.6903 \bullet Cl + 0.5482 \bullet Si + 4.2844 \bullet OC \quad (A.4)$$

$$\theta FC = 0.46 \bullet Cl + 0.3045 \bullet Si + 2.0703 \bullet OC \quad (A.5)$$

$$\theta WP = 0.3624 \bullet Cl + 0.117 \bullet Si + 1.6054 \bullet OC \quad (A.6)$$

Batjes FC@1.7pF:

$$\theta PS = 0.6903 \bullet Cl + 0.5482 \bullet Si + 4.2844 \bullet OC \quad (A.7)$$

$$\theta FC = 0.6681 \bullet Cl + 0.2614 \bullet Si + 2.215 \bullet OC \quad (A.8)$$

$$\theta WP = 0.3624 \bullet Cl + 0.117 \bullet Si + 1.6054 \bullet OC \quad (A.9)$$

Where:

θPS: water content at saturation or pore space (fraction of 1); θFC: water content at field capacity (fraction of 1); θWP: water content at wilting point (fraction of 1); Cl: clay content (%); OC: organic carbon content (%); Si: silt content (%); BD: bulk density (g cm^{-3}).

Data availability

Data will be made available on request.

References

Al-Shammary, A.A.G., Kouzani, A.Z., Kaynak, A., Khoo, S.Y., Norton, M., Gates, W., 2018. Soil bulk density estimation methods: a review. Pedosphere 28 (4), 581–596. https://doi.org/10.1016/S1002-0160(18)60034-7.

Bagnall, D.K., Morgan, C.L.S., Cope, M., Bean, G.M., Cappellazzi, S., Greub, K., et al., 2022. Carbon-sensitive pedotransfer functions for plant available water. Soil Sci. Soc. Am. J. 86 (3), 612–629. https://doi.org/10.1002/saj2.20395.

Batjes, N., 1996. Development of a world data set of soil water retention properties using pedotransfer rules. Geoderma 71 (1-2), 31–52.

Beaudette, D., Reid, R., & Skaggs, T., 2024, ROSETTA Model API, ⟨https://ncss-tech.github.io/AQP/soilDB/ROSETTA-API.html⟩.

Burt, R., 1996. In: Burt, R. (Ed.), Soil Survey Laboratory Methods Manual. Scientific Publishers - USDA.

Chen, Z., Xue, J., Wang, Z., Zhou, Y., Deng, X., Liu, F., et al., 2024. Ensemble modelling-based pedotransfer functions for predicting soil bulk density in China. Geoderma 448, 116969. https://doi.org/10.1016/j.geoderma.2024.116969.

Chirico, G.B., Medina, H., Romano, N., 2010. Functional evaluation of PTF prediction uncertainty: an application at hillslope scale. Geoderma 155 (3-4), 193–202.

Correndo, A., 2024, Regression performance metrics and indices, ⟨https://cran.r-project.org/web/packages/metrica/vignettes/available_metrics_regression.html⟩.

Decharme, B., Boone, A., Delire, C., Noilhan, J., 2011. Local evaluation of the Interaction between Soil Biosphere Atmosphere soil multilayer diffusion scheme using four pedotransfer functions. J. Geophys. Res. Atmos. 116 (D20).

Eckelmann, W., Sponagel, H., Grottenthaler, W., Hartmann, K.-J., Hartwich, R., Janetzko, P., et al., 2005. Bodenkundliche Kartieranleitung.-5. verbesserte und erweiterte-Auflage (Manual of soil mapping. 5th Ed. - KA5). Schweizerbart Science Publishers, Stuttgart, Germany.

El Sharif, H., Wang, J., Georgakakos, A.P., 2015. Modeling regional crop yield and irrigation demand using SMAP type of soil moisture data. J. Hydrometeorol. 16 (2), 904–916.

Emerman, S.H., 1995. The tipping bucket equations as a model for macropore flow. J. Hydrol. 171 (1-2), 23–47.

Evett, S.R., Stone, K.C., Schwartz, R.C., O'Shaughnessy, S.A., Colaizzi, P.D., Anderson, S. K., et al., 2019. Resolving discrepancies between laboratory-determined field capacity values and field water content observations: implications for irrigation management. Irrig. Sci. 37 (6), 751–759. https://doi.org/10.1007/s00271-019-00644-4.

Givi, J., Prasher, S., Patel, R., 2004. Evaluation of pedotransfer functions in predicting the soil water contents at field capacity and wilting point. Agric. Water Manag. 70 (2), 83–96.

Groh, J., Diamantopoulos, E., Duan, X., Ewert, F., Herbst, M., Holbak, M., et al., 2020. Crop growth and soil water fluxes at erosion-affected arable sites: using weighing lysimeter data for model intercomparison. Vadose Zone J. 19 (1), e20058. https://doi.org/10.1002/vzj2.20058.

Groh, J., Stumpp, C., Lücke, A., Pütz, T., Vanderborght, J., Vereecken, H., 2018. Inverse estimation of soil hydraulic and transport parameters of layered soils from water stable isotope and lysimeter data. Vadose Zone J. 17 (1), 170168. https://doi.org/10.2136/vzj2017.09.0168.

Guber, A.K., Pachepsky, Y.A., van Genuchten, M.T., Simunek, J., Jacques, D., Nemes, A., et al., 2009. Multimodel simulation of water flow in a field soil using pedotransfer functions. Vadose Zone J. 8 (1), 1–10. https://doi.org/10.2136/vzj2007.0144.

Heil, K., Heinemann, P., Schmidhalter, U., 2018. Modeling the effects of soil variability, topography, and management on the yield of barley. Front. Environ. Sci. 6. https://doi.org/10.3389/fenvs.2018.00146.

Herbrich, M., Gerke, H.H., 2017. Scales of water retention dynamics observed in eroded luvisols from an arable postglacial soil landscape. Vadose Zone J. 16 (10). https://doi.org/10.2136/vzj2017.01.0003.

Hyndman, R.J., Koehler, A.B., 2006. Another look at measures of forecast accuracy. Int. J. Forecast. 22 (4), 679–688.

Jarvis, N., Larsbo, M., Lewan, E., Garré, S., 2022. Improved descriptions of soil hydrology in crop models: the elephant in the room? Agric. Syst. 202, 103477. https://doi.org/10.1016/j.agsy.2022.103477.

Jensen, M.E., Burman, R.D., Allen, R.G., 1990. Evapotranspiration and irrigation water requirements: a manual. ASCE Man. Rep. Eng. Pract. (USA) 70.
Kar, G., Chattaraj, S., Kumar, A., 2013. Pedo-transfer functions for determining soil water retention and assessing their utility in simulation model for predicting rice growth and yield. J. Indian Soc. Soil Sci. 61 (4), 300–310.
Kersebaum, K.C., 2007. Modelling nitrogen dynamics in soil–crop systems with HERMES. Nutr. Cycl. Agroecosyst. 77 (1), 39–52. https://doi.org/10.1007/s10705-006-9044-8.
Kersebaum, K.C., 2011. Special features of the HERMES model and additional procedures for parameterization, calibration, validation, and applications. In: L.R.a.M., Ahuja, L. (Eds.), Methods of Introducing System Models into Agricultural Research. ASA, Madison, Wisconsin, USA, pp. 65–94. https://doi.org/10.2134/advagricsystmodel2.c2.
Kersebaum, K.C., Wallor, E., Lorenz, K., Beaudoin, N., Constantin, J., Wendroth, O., 2019. Modeling cropping systems with HERMES–Model capability, deficits and data requirements. Bridg. Discip. Synth. Soil Plant Process. 103–126. https://doi.org/10.2134/advagricsystmodel8.2017.0005.
Kirchner, J.W., 2006. Getting the right answers for the right reasons: linking measurements, analyses, and models to advance the science of hydrology. Water Resour. Res. 42 (3). https://doi.org/10.1029/2005WR004362.
Krevh, V., Groh, J., Weihermüller, L., Filipović, L., Defterdarović, J., Kovač, Z., et al., 2023. Investigation of hillslope vineyard soil water dynamics using field measurements and numerical modeling. Water 15 (4), 820.
Liebhard, G., Klik, A., Neugschwandtner, R.W., Nolz, R., 2022. Effects of tillage systems on soil water distribution, crop development, and evaporation and transpiration rates of soybean. Agric. Water Manag. 269, 107719. https://doi.org/10.1016/j.agwat.2022.107719.
Lu, Y., Chibarabada, T.P., Ziliani, M.G., Onema, J.-M.K., McCabe, M.F., Sheffield, J., 2021. Assimilation of soil moisture and canopy cover data improves maize simulation using an under-calibrated crop model. Agric. Water Manag. 252, 106884. https://doi.org/10.1016/j.agwat.2021.106884.
Mirschel, W., Wenkel, K.-O., 2007. Modelling Soil–crop Interactions with AGROSIM Model Family. Modelling Water and Nutrient Dynamics in Soil–crop Systems. Springer Netherlands.
Moeys, J., Larsbo, M., Bergström, L., Brown, C.D., Coquet, Y., Jarvis, N., 2012. Functional test of pedotransfer functions to predict water flow and solute transport with the dual-permeability model MACRO. Hydrol. Earth Syst. Sci. 16 (7), 2069–2083.
Montzka, C., Herbst, M., Weihermüller, L., Verhoef, A., Vereecken, H., 2017. A global data set of soil hydraulic properties and sub-grid variability of soil water retention and hydraulic conductivity curves. Earth Syst. Sci. Data 9 (2), 529–543. https://doi.org/10.5194/essd-9-529-2017.
Nasta, P., Szabó, B., Romano, N., 2021. Evaluation of pedotransfer functions for predicting soil hydraulic properties: a voyage from regional to field scales across Europe. J. Hydrol. Reg. Stud. 37, 100903. https://doi.org/10.1016/j.ejrh.2021.100903.
Pachepsky, Y., van Genuchten, M.T., 2011. Pedotransfer functions. Encycl. Agrophys. 556–561.
Panagos, P., De Rosa, D., Liakos, L., Labouyrie, M., Borrelli, P., Ballabio, C., 2024. Soil bulk density assessment in Europe. Agric. Ecosyst. Environ. 364, 108907. https://doi.org/10.1016/j.agee.2024.108907.
Paschalis, A., Bonetti, S., Guo, Y., Fatichi, S., 2022. On the uncertainty induced by pedotransfer functions in terrestrial biosphere modeling. Water Resour. Res. 58 (9), e2021WR031871. https://doi.org/10.1029/2021WR031871.
Pütz, T., Kiese, R., Wollschläger, U., Groh, J., Rupp, H., Zacharias, S., et al., 2016. TERENO-SOILCan: a lysimeter-network in Germany observing soil processes and plant diversity influenced by climate change. Environ. Earth Sci. 75 (18), 1242. https://doi.org/10.1007/s12665-016-6031-5.
Ramcharan, A., Hengl, T., Beaudette, D., Wills, S., 2017. A soil bulk density pedotransfer function based on machine learning: a case study with the NCSS soil characterization database. Soil Sci. Soc. Am. J. 81 (6), 1279–1287. https://doi.org/10.2136/sssaj2016.12.0421.
Ramos, T.B., Darouich, H., Gonçalves, M.C., 2023. Development and functional evaluation of pedotransfer functions for estimating soil hydraulic properties in Portuguese soils: implications for soil water dynamics. Geoderma Reg. 35, e00717. https://doi.org/10.1016/j.geodrs.2023.e00717.
Reynolds, W.D., 2018. An analytic description of field capacity and its application in crop production. Geoderma 326, 56–67. https://doi.org/10.1016/j.geoderma.2018.04.007.
Schaap, M.G., Zhang, Y., Nemes, A., 2023. Pedotransfer functions and their application to soil water dynamics. In: Goss, M.J., Oliver, M. (Eds.), Encyclopedia of Soils in the Environment (Second Edition). Oxford: Academic Press, pp. 642–654. https://doi.org/10.1016/B978-0-12-822974-3.00210-X.
Schübl, M., Brunetti, G., Fuchs, G., Stumpp, C., 2023. Estimating vadose zone water fluxes from soil water monitoring data: a comprehensive field study in Austria. Hydrol. Earth Syst. Sci. 27 (7), 1431–1455. https://doi.org/10.5194/hess-27-1431-2023.
Smith, M., Allen, R., & Pereira, L., 1998. Revised FAO methodology for crop-water requirements,
Stenger, R., Priesack, E., Barkle, G., Sperr, C., 1999. Expert-N a tool for simulating nitrogen and carbon dynamics in the soil-plant-atmosphere system, pp. 19–28.
Sun, X.-L., Wang, X.-Q., Wang, H.-L., 2019. Comparison of estimated soil bulk density using proximal soil sensing and pedotransfer functions. J. Hydrol. 579, 124227. https://doi.org/10.1016/j.jhydrol.2019.124227.
Szabó, B., Weynants, M., Weber, T.K., 2021. Updated European hydraulic pedotransfer functions with communicated uncertainties in the predicted variables (euptfv2). Geosci. Model Dev. 14 (1), 151–175.
Tóth, B., Weynants, M., Nemes, A., Makó, A., Bilas, G., Tóth, G., 2015. New generation of hydraulic pedotransfer functions for Europe. Eur. J. Soil Sci. 66 (1), 226–238.
Van Looy, K., Bouma, J., Herbst, M., Koestel, J., Minasny, B., Mishra, U., et al., 2017. Pedotransfer functions in Earth system science: challenges and perspectives. Rev. Geophys. 55 (4), 1199–1256.
Vereecken, H., Huisman, J.A., Bogena, H., Vanderborght, J., Vrugt, J.A., Hopmans, J.W., 2008. On the value of soil moisture measurements in vadose zone hydrology: a review. Water Resour. Res. 44 (4). https://doi.org/10.1029/2008WR006829.
Vereecken, H., Schnepf, A., Hopmans, J.W., Javaux, M., Or, D., Roose, T., et al., 2016. Modeling soil processes: review, key challenges, and new perspectives. Vadose Zone J. 15 (5).
Wagner, B., Tarnawski, V., Hennings, V., Müller, U., Wessolek, G., Plagge, R., 2001. Evaluation of pedo-transfer functions for unsaturated soil hydraulic conductivity using an independent data set. Geoderma 102 (3-4), 275–297.
Wallor, E., Kersebaum, K.-C., Lorenz, K., Gebbers, R., 2019. Soil state variables in space and time: first steps towards linking proximal soil sensing and process modelling. Precis. Agric. 20, 313–334.
Walter, K., Don, A., Tiemeyer, B., Freibauer, A., 2016. Determining soil bulk density for carbon stock calculations: a systematic method comparison. Soil Sci. Soc. Am. J. 80 (3), 579. https://doi.org/10.2136/sssaj2015.11.0407.
Wankmüller, F.J.P., Delval, L., Lehmann, P., Baur, M.J., Cecere, A., Wolf, S., et al., 2024. Global influence of soil texture on ecosystem water limitation. Nature. https://doi.org/10.1038/s41586-024-08089-2.
Weber, T.K.D., Weihermüller, L., Nemes, A., Bechtold, M., Degré, A., Diamantopoulos, E., et al., 2024. Hydro-pedotransfer functions: a roadmap for future development. Hydrol. Earth Syst. Sci. 28 (14), 3391–3433. https://doi.org/10.5194/hess-28-3391-2024.
Weihermüller, L., Lehmann, P., Herbst, M., Rahmati, M., Verhoef, A., Or, D., et al., 2021. Choice of pedotransfer functions matters when simulating soil water balance fluxes. J. Adv. Model. Earth Syst. 13 (3), e2020MS002404. https://doi.org/10.1029/2020MS002404.
Wendling, U., Schellin, H.-G., Thomä, M., 1991. Bereitstellung von täglichen Informationen zum Wasserhaushalt des Bodens für die Zwecke der agrarmeteorologischen Beratung. Z. F. üR. Meteorol. 41 (6), 468–475.
Wiecheteck, L.H., Giarola, N.F.B., de Lima, R.P., Tormena, C.A., Torres, L.C., de Paula, A. L., 2020. Comparing the classical permanent wilting point concept of soil (−15,000 hPa) to biological wilting of wheat and barley plants under contrasting soil textures. Agric. Water Manag. 230, 105965. https://doi.org/10.1016/j.agwat.2019.105965.
Xu, L., He, N., Yu, G., 2016. Methods of evaluating soil bulk density: impact on estimating large scale soil organic carbon storage. Catena 144, 94–101. https://doi.org/10.1016/j.catena.2016.05.001.
Zhang, Y., Schaap, M.G., 2017. Weighted recalibration of the Rosetta pedotransfer model with improved estimates of hydraulic parameter distributions and summary statistics (Rosetta3). J. Hydrol. 547, 39–53.